INCREASING COTTON PRODUCT/WASTE VALUE THROUGH NEW USE

DEVELOPMENT

A Thesis
Submitted to the Graduate Faculty
of the
North Dakota State University
of Agriculture and Applied Science

By

Damian Lance Mohawk

In Partial Fulfillment of the Requirements
for the Degree of
MASTER OF SCIENCE

Major Program:
Materials and Nanotechnology

June 2021

Fargo, North Dakota

North Dakota State University
Graduate School

Title

INCREASING COTTON PRODUCT/WASTE VALUE THROUGH NEW
USE DEVELOPMENT

By

Damian Lance Mohawk

The Supervisory Committee certifies that this ***disquisition*** complies with North Dakota

State University's regulations and meets the accepted standards for the degree of

Master of Science

SUPERVISORY COMMITTEE:

Dr. Long Jiang

Chair

Dr. Ali Amiri

Dr. Chad Ulven

Dr. Dean Webster

Approved:

07/07/2021	Dr. Erik Hobbie
Date	Department Chair

ABSTRACT

Cotton products have been used for centuries with relatively low value and their ubiquitous use generating large quantities of waste materials. This research's goal was to develop new uses for waste cotton fiber and cottonseed oil to increase their value and create new biobased products. Cotton fabric was treated using a furnace and autoclave under different gas environments and temperatures to study chemical and physical effects before and after epoxy composite incorporation. Findings showed relatively low temperature treatments possess effective reinforcement due to improved interfacial bonding. A high treatment temperature led to structural damages of fibers and resulted in reduced reinforcement. Acrylated and dimethacrylated cottonseed oil produced resins that could be readily crosslinked. Mechanical properties of cured cottonseed oil-based formulations showed a slightly lower strength than soybean oil-based and commercial resin due to its lower functionality. Stereolithography 3D printing of the resin was investigated and complex objects were manufactured.

ACKNOWLEDGMENTS

TABLE OF CONTENTS

LIST OF TABLES

LIST OF FIGURES

LIST OF ABBREVIATIONS

AECO…………………………………………………….Acrylated Epoxidized Cottonseed Oil

AESO…………………………………………………….Acrylated Epoxidized Cottonseed Oil

ASTM……………………………………………………American Society for Testing Materials

ATR………………………………………………………...Attenuated Total Reflection

CSO…………………………………………………………Cottonseed Oil

DMA……………………………………………………….Dynamic Mechanical Analysis

DMECO……………………………………………..Dimethacrylated Epoxidized Cottonseed Oil

ECO…………………...………………………………...Epoxidized Cottonseed Oil

EDS…………………………………………………Energy Dispersive X-Ray Spectroscopy

FTIR…………………………………………………………...Fourier-Transform Infrared

HDDA…………………………………………………….………1,6-Hexanediol Diacrylate

LED………………………………………………………………….Light Emitting Diode

PETA………………………………………………………Pentaerythritol Tetraacrylate

SEM……………………………………………………………..Scanning Electron Microscopy

SLA……………………………………………………..Stereolithography Apparatus

TGA……………………………………………………………Thermogravimetric Analyzer

TMPTA…………………………………………………...Trimethylolpropane Triacrylate

TPGDA……………………………………………………Tri(Propylene Glycol) Diacrylate

UV………………………………………………………………………..Ultraviolent

XRD………………………………………………………………….X-Ray Diffraction

INTRODUCTION

Problem Statement

Cotton is the most abundantly grown textile crop around the globe and has been a revolutionizing material throughout human history.[1] First uses of cotton date back to as early as 3000 B.C. in what is now Pakistan and India for use as loose fabric and cloth.[2] Modern cultivation and fabrication however is an ever-growing global market with research branching into all sectors of industry. Like most industries however, waste is nearly always generated and requires some form of standard or specialized disposal that can be environmentally harmful, financially draining, or generally a nuisance. In cottons case, many different forms of waste are generated such as woven fabric, cotton thread, polycotton, cottonseed oil, and bulk raw cotton. These products can become waste either through gradual consumer degradation or industrial waste/byproducts and end up in landfills and burn pits.

Research Motivation

Repurposing end-of-life cotton products, such as cotton fabrics, have seen a great deal of attention in research with many groups looking to recycle post-consumer fabrics. Untreated fabrics have been incorporated into polymer matrices as reinforcement to improve mechanical properties. Limitations however have been seen with poor interfacial adhesion between the polymer and fiber surface due to few reactive sights for bonding.[3] To counter this, varying chemical treatments have been trialed on cotton fabric to improve adhesion to polymer matrices with promising results. However, most treatments involve a strong chemical acid or base to functionalize the surface which creates chemical waste.[4,5] One method for the treatment of cotton fabric stands out which is thermal treatment to modify the cellulose structure. Early works have proven this to be an environmentally friendly treatment for cotton fabric and cellulose materials

1

alike with potential for improvement to mechanical and electrical properties.[6,7] By incorporation of thermally treated cotton fabric into composites, it may be ideal for expanding the product's potential. These studies collectively show that further research into reuse of end-of-life/waste cotton is still needed to find environmentally friendly, affordable, and effective solutions for manufacturing the ideal cotton and polymer composites.

Cottonseed oil (CSO) is a common cooking oil in many parts of the world with it being a typical ingredient in dressings, condiments, and snacks. Many studies have sought to find new value-added uses for CSO through a multitude of ways. Most prominently is the transesterification of CSO to form fatty acids for biodiesels. While the high yield makes the process appear ideal, catalyst costs hinder large scale production.[8] Others have studied the potential of maleic acid treated CSO as a plasticizer in poly(lactic acid). It was found that the incorporation of the maleinized CSO could increase the maximum elongation with minimal loss to the glass transition temperature and noticeable accelerations in the decomposition rate with increasing oil content.[9] While this application is promising, the quantity of oil used is small, meaning even at an industrial scale not much oil is needed to be recycled for this purpose. Others have instead attempted epoxidizing the CSO to form epoxidized cottonseed oil (ECO) which can be crosslinked to form solid structures and films.[10] Results have shown comparable potential to similar products available on the market such as epoxidized soybean oil (ESO). While continued research and gradual adoption into the biofuel market will come, studies are proving value in the exploration of crosslinking modified versions of CSO into practical structures. Further study must be sought to assist in consuming the immense quantity of CSO produced annually and to add further value to the product.

Research Objectives

Since many current recycling/upcycling methods and new uses of cotton products involve either costly constituents, the formation of hazardous byproducts, or generally fall short of their true potential, further investigation into new recycling methods and new uses of cotton products is necessary so that more environmentally friendly and affordable solutions can be developed. The two primary objectives of this research are as follows:

- Development of thermally treated cotton fabric as composite reinforcement

- Development of CSO-based resin for 3D printing and traditional plastic molding

This thesis consists of five chapters. Chapter 1 addresses waste cotton fabric and low value cottonseed oil as problems at hand with the motivation to develop value adding applications such as treated-cotton composites and 3D printable resins. Chapter 2 gives background into cotton fiber and its previous work under thermal treatment and as composite reinforcement as well as the background of cottonseed oil and its acrylated epoxidized form. Chapter 3 explores a technique for adding value to waste cotton fabric by thermal treatment in both furnace and autoclave environments under various conditions (temperature and gas) for the incorporation as reinforcement in cotton/epoxy composites. Chapter 4 introduces a novel processing and post-processing technique for CSO by repurposing the acrylated and epoxidized form of the oil for SLA 3D printing through the incorporation of photo and thermal initiators as well as multiple reactive diluents at various amounts to be crosslinked into complex objects. Chapter 5 recites the rationality for these studies and concludes the potential viability of each application to address their problems along with a plan of future work to pursue.

BACKGROUND

Cotton

Since its first cultivation in early B.C., cotton production has grown with human evolution to become one of the most abundantly harvested textile fibers worldwide. According to the USDA, cotton production worldwide averaged around 120 million bales in the 2019-2020 year, equating to 24 million tons, with the majority deriving from India, China, and the United States respectively.[11] Demand grows annually as application development continues from traditionally simple clothes and blankets to filters, bandages, and even fishing nets. Standard cotton fabrics are comprised of countless fibers which are roughly 94 wt% cellulose with the remaining 6 wt% being a distribution of pectin, wax, protein, ash, and impurities.[12] These components form the cuticle, primary, winding, secondary, and lumen layers of the fiber as seen in *Figure 1* with each having unique orientation angles forming an overall helical shape.[13,14] Between and throughout these layers exists a porous structure which quickly swells when in contact with water, attributing to cotton fibers natural hydrophilicity.[15] Under dry conditions, fibers are seen to collapse inward on themselves to form a ribbon shape rather than a tubular shape when hydrated.
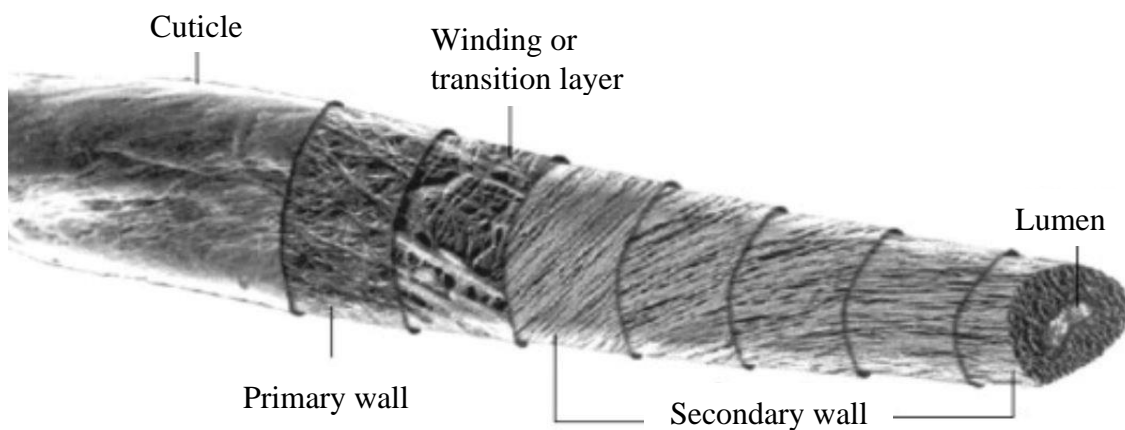
Figure 1. Multilayer internal structure of cotton fiber.[14]

After processing through bleaching and scouring, the surface pectin, wax, and impurities in the cuticle are removed leaving the fibers as nearly 99% cellulose. The varying orientations of cellulose attribute to the fibers natural strength with increasing crystallinity indexes from 30-70% towards the center.[12,15] Being that most fresh cotton fibers have a predetermined purpose, investigation into purposes for their end-of-life products needs evaluation. Through varying solvent separation methods, regenerated cotton fibers can be produced and wet-spun into new products. Promising mechanical properties and fibril characteristics both alone and when blended with varying pulps have been found.[4,16] The process however involves chopping the fibers which decreases the fibers aspect ratio and subsequently causes a loss in potential strength of the recycled products on top of hazardous wastes being generated from the solvent processing. Because of this, further research must be sought for environmentally friendly treatments for regeneration of cotton fibers or new repurposing applications that eliminated the need for hazardous treatment.

Cotton Fiber as Composite Reinforcement

Reinforcement in composites is one of the most common uses for fibers in today's world with applications ranging from super cars to bulletproof barriers to bathtubs. Each type of fiber has its own purposes depending on its characteristics and properties which is why cotton is generally used for affordable, light weight, and low strength applications. Being that a majority of end-of-life cotton is in fabric form, it can be rationalized that it is already in its ideal form for composite incorporation. Untreated fabrics have been incorporated into polymer matrices such as polyesters and polypropylenes as reinforcement with findings showing near double sliding wear resistance and increased ultimate tensile strength compared to the neat polymers.[3,17] Other studies have explored the fracture toughness and delamination characteristics of cotton epoxy composites at different modes and found strengths in specific orientations that are comparable to

5

carbon fiber and glass reinforced composites.[18] Examination has shown though that untreated

cotton fabrics have very poor interfacial adhesion to most polymer matrices. This means applied

stresses are not being distributed to the fibers but are rather being absorbed by the polymer which

promises a reduction in composite properties and premature failure.

To improve interfacial adhesion of cotton in polymer matrices, many different methods

have been implemented. Reduced graphene oxide has been applied to cotton fibers before

incorporation into epoxy with results showing improvements to tensile, flexural, and impact

strengths. These improvements were attributed to the graphene's numerous oxygen-based

functional groups that can react with both the cellulose of the cotton and the epoxy.[19] Others

have used oligomers containing epoxy functional groups have been deposited on cotton fiber's

surface before composite incorporation. Since the epoxy groups can react with both the hydroxyl

groups of the cotton as well as the hydroxyl and carboxyl groups of different renewable

polymers, this oligomer can essentially act as a coupling agent between the two.[20] Findings

showed improvements of elastic modulus and ultimate stress in PLA which were attributed to

improved adhesion and lessened fiber pullout observed in SEM.[20] Cotton's natural hydrophilicity

also attributes to its poor adhesion to polymers which is why attempts to functionalize cotton

fabrics surface with palmitic acid using zinc and aluminum hydroxide at varying concentrations

and durations have been trialed.[21] Findings have shown contact angles upwards of 140° which

indicates outstanding hydrophobicity. Sodium hydroxide at varying concentrations has also been

used to functionalize cotton for improved interfacial adhesion with results displaying

improvement in elastic modulus up to 70% and tensile strength by up to 400%.[5] Even the

incorporation of zinc oxide nanoparticles and polyvinylsilsesquioxane as a coating to form

composites from cotton fibers have been studied in tandem to functionalize the surface with

nano-structures and lower the overall surface energy, respectively. While findings showed extreme hydrophobicity and increased mechanical properties after treatment compared to pristine cotton fabric, deterioration in mechanical strength was seen with increasing zinc oxide content.[22] These direct and indirect repurposes exhibit the effectiveness in utilizing cotton fabric for its natural physical properties in composites as well as the vast potential for modification. However, they each involve either the use or addition of chemicals or compounds that can be expensive or harmful to the environment.

Thermally Treated Cotton

Thermally treating cotton and cotton products is the process of dehydrating, pyrolyzing, or calcinating at varying temperatures in highly controlled and potentially inert environments to reduce the oxygen content in the cellulose and induce decarboxylation. Autoclaving cellulose products like cotton is a commonly studied method of treatment for a variety of reasons including versatility and affordability. Findings have shown that during treatment, the cellulose that makes up cotton degrades into glucose and fructose which then evolve into further species.[23] This process splits a crossroad between solid material and liquid phase making environment and temperature critical. Studies have shown that the varying walls degrade in sequence of most amorphous to most crystalline with amorphous and crystalline cellulose beginning degradation at 150°C and 180°C, respectively.[23,24] Interest has been seen in increasing surface area of cellulose by autoclaving it in a water and HCl solution with findings showing potential for dramatic improvement upwards of 386m^2/g. Certain durations and solutions however only produced surface areas near 100m^2/g.[25] Some studies have gone as far as to convert cotton textile into solid fuels and bio-oils using surfactants as catalysts with findings showing enhancement in both productions and fuel properties. Unfortunately, the creation of bio-oil consumes the production of solid fuel making it in need of further study.[26]

Furnace treatment of cellulose is another common method with various temperatures and gas environments. Increasing treatment temperatures correlate to increasing weight percentage carbon in the treated fabrics, which widens the range of applications due to high carbon content materials having useful electrical and mechanical properties that suit a variety of needs.[27] Previous studies have sought to carbonize cotton fabric through thermal treatment with a graphene coating to be used as wearable and flexible pressure sensors. Sensors showed a hysteresis as low as 3.39% and a sensitivity as high as 74.8 kPa-1, making them suitable for detecting the most subtle of differences.[6,28] Others have explored usage of carbonized cotton as substrates or electrodes in super-capacitors due to its high carbon content and flexibility. One group conducted nitrogen doping of carbonized cotton by carbonizing cotton in a flowing mixture of Ar and NH_3. The doping led to increased surface area and wettability of the carbonize cotton and imparted pseudo-capacitive effect to the material, resulting in substantially improved specific capacitance and energy/power density of the sample super-capacitor.[29,30] Finally, even strains improvements upwards of 140% could be obtained with treated cotton fabric, making its modification a potentially low-cost alternative to carbon fiber with effective usage in compression, tension, torsion, and bend sensing applications.[6,28]

All these studies together prove that the thermal treatment of cotton fabrics is not just achievable but potentially an industry in and of itself. While limitations still hinder the adoption of some solutions, there is more potential yet to be exploited from cotton fabric.

Cottonseed Oil

Annual production of cottonseed oil is overlooked by most due to its few purposes, yet estimates place production at around five-million metric tons.[11] Extraction of the oil from the cottonseed can be done in a variety of ways including supercritical CO_2, n-hexane solvent and

their mixtures with other solvents such as ethanol, acetone, heptane, etc. which extracts the 18-25% oil content in the seeds.[31,32] When extracted, the oil typically contains a harmful amount of gossypol which is naturally produced by the cotton plant to act as an insect repellent. Gossypol can be very harmful if consumed in large quantities which means refinement through microbial treatment, bleaching, and deodorizing is required.[33] Because of these extra steps required to make CSO safe for human and animal consumption in food or feedstock, it has seen slow adoption into this market compared to other plant-based oils. Like most organic oils, a single glycerol group and three attached fatty acids comprise the oils structure as seen in *Figure 2*. Most common in CSO are linoleic, palmitic, and oleic acid which consist of 52.89%, 25.39%, and 16.35% respectively with remaining small amounts of stearic, myristic, palmitoleic, and linolenic acid.[34] A majority of the fatty acids are polyunsaturated with some monounsaturated and saturated which is common to plant-based oils. Many studies have sought to recycle CSO to form biodiesels and have obtained yields greater than 90% with emission characteristics showing both carbon monoxide and nitrogen oxide emission decreases alongside satisfying ASTM fuel standards.[8,35] To replace expensive catalysts some has investigated recycled egg shells as a catalyst and found that the calcium oxide generated works effectively compared to chemically synthesized versions.[35]
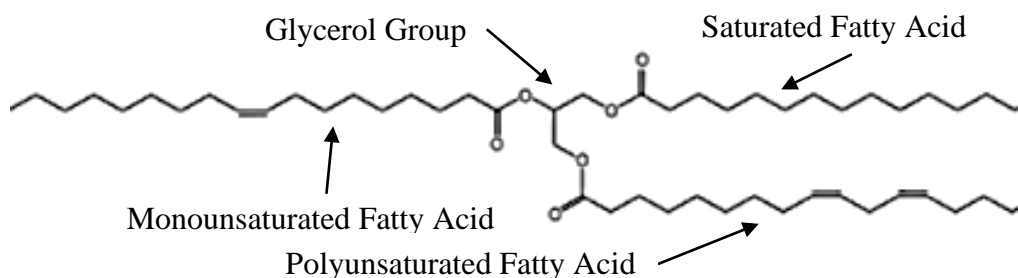
Figure 2. Molecular structure of cottonseed oil.

Modified Cottonseed Oil

Of the studies to repurpose CSO, the most interesting are those involving the epoxidation of cottonseed oil using catalysts on the fatty acids so that the oil can be readily functionalized to the desired state. As shown in *Figure 3*, epoxidation can be accomplished through treatment of CSO with formic acid and hydrogen peroxide which transforms the unsaturated double bonds of the fatty acids into epoxide groups. Functionality makes incorporation into poly(lactic acid) and poly(vinyl chloride) as a plasticizer to form plastisol's a possibility. Incorporating the ECO into poly(lactic acid) displays good homogeneity with around 2.5 wt% ECO and slight phase separation at upwards of 10 wt% ECO. Regardless, the 10 wt% ECO formulations improved elongation by 110.5% and decrease the glass transition by 6°C.[36] In poly(vinyl chloride), incorporation upwards of 70 wt% ECO saw homogenous phases and over 150% improvements in elongation.[37] With curability into complex polymers certain, its suggested that modified CSO could be used in replacement of epoxidized soybean oils. Many new studies show the feasibility of structure formation and SLA 3D printing using varieties of modified soybean oils. Urethane epoxidized soybean oils have shown promise as an additive into epoxy acrylate with SLA 3D printed structures showing clear homogeneity and improved tensile strength without loss in elongation. However, contents of greater than 20 wt% soybean oil was found to increase the resins viscosity above a suitable level for 3D printing.[38] Higher content formulations (64.8 to 99.7 wt%) have been trialed with acrylated epoxidized soybean oil for SLA 3D printing with findings showing increased glass transition and maximum degradation temperatures as well as increased thermal stability in comparison to standard 3D printed and UV lamp cured objects.[39]
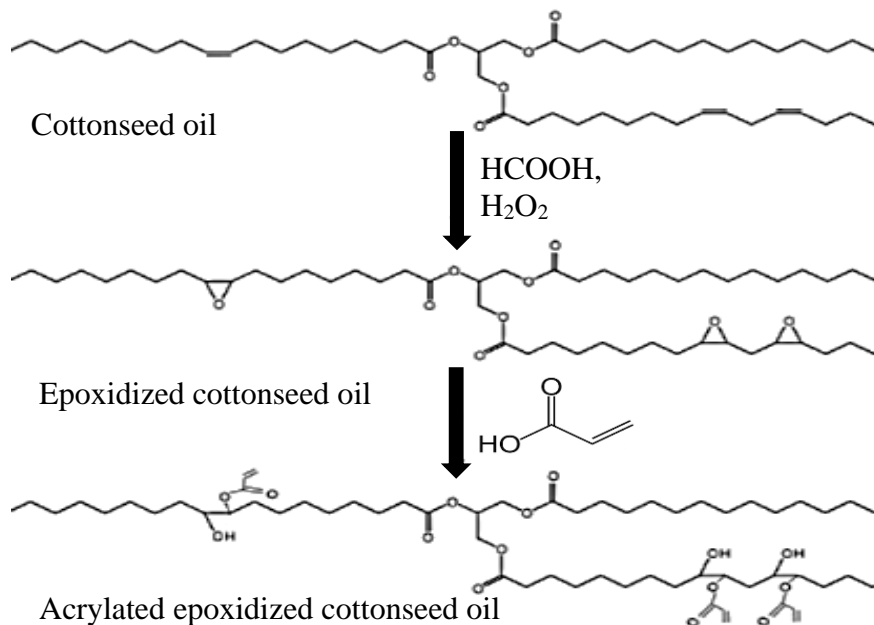
Figure 3. Epoxidation and acrylation of cottonseed oil.

Similar forms of CSO can be synthesized by going one step further with the ECO. Through the incorporation of acrylic acid, a single bond on each epoxide group is broken to form an equal number of both hydroxyl and acrylate groups as seen in *Figure 3*. In theory, this acrylation step doubles the potential reactive sites on each oil molecule giving it the ability to form improved crosslinking in a polymer matrix. Modified into AECO, CSO has the potential to follow suit with soybean oil to be photo cured into complex structures through SLA 3D printing. Preliminary studies have shown that simple structures can be formed from crosslinked ECO with findings showing that up to 98.3% conversion of the unsaturated fatty acids could be obtained with an oxirane oxygen index as low as 5.32% comparable to epoxidized soybean oil.[9] While more efficient and environmentally friendly approaches for the modification steps are being explored, further research must be done into applications for the end-product to justify the future work. All these studies collectively prove that the recycling of cotton products is not just achievable but potentially an industry in and of itself. While limitations still hinder the adoption of some solutions, there is more potential yet to be exploited from cotton products.

THERMAL TREATMENTS OF COTTON FOR ENHANCED REINFORCEMENT IN COTTON/EPOXY COMPOSITES

Introduction

Thermal treatment of cotton fiber can be accomplished through several processes, at a variety of temperatures, and in almost any environment. In this chapter, two forms of heat-treatment, i.e., furnace and hydrothermal treatment, were carried out under different conditions. Furnace treatment allows for a large range of temperatures to be trialed in different gas environments (air and N_2 in this study) while autoclave treatment involves high pressure water vapor under moderate temperatures. Cotton undergoes different chemical reactions in these two processes and the treated cotton exhibits different properties. For these reasons, specific temperatures and environments were chosen for direct comparison of the two methods while other combinations of parameters were chosen to better understand the potential benefits and limitations of each method individually.

Materials used for these trials included jersey woven cotton fabric produced from scoured and bleached cotton fiber provided by Cotton Incorporated and epoxy resin (Clearcast 7000) manufactured by Superior Plastics. This polyamine epoxy is formed from a 1:1 ratio of proprietary blends containing 2,2'-[(1-methylethylidene)bis(4,1-phenyleneoxy-methylene)]bisoxirane and polyoxypropylene diamine which act as the epoxide functional resin and difunctional amine hardener, respectively. Choice of this epoxy was for its versatility, clarity, and self-degassing properties as well as commonality. Analysis was carried out on both treated cotton fabric as well as epoxy/treated fabric composites using techniques such as tensile testing, TGA, FTIR, SEM, EDS, and XRD. From the experimental results, physical and

mechanical properties of the treated cotton and the epoxy/cotton composites were analyzed. Important conclusions were drawn and directions of future study were shown.

Fabric Thermal Treatment

Temperatures trialed ranged from 140°C to 1000°C depending on the technique and environment chosen since for temperatures at or above 600°C an inert environment is required to inhibit combustion. Thermal treatment of organic polymers at high temperatures can generate carbon-rich structures, such is the process for transforming a polyacrylonitrile precursor into carbon fiber which have vast potential for countless applications. For this reason, high temperature treatments (600°C -1000°C) must be investigated for their potential to transform cotton fabrics into carbon-rich structures. At low temperatures, cellulose's structure still undergoes chemical transformations, and its morphology can be altered. For this reason, low temperature treatments (140°C -210°C) require research to determine their potential benefits. Furnace heat-treatment involved an Across International STF1200 quartz-tube furnace. Cotton samples were rolled gently before being set in a 4 by 1.5-inch alumina boat and placed directly in the center of the tube furnace. Once sealed and activated, the furnace was purged with a steady stream of gas (N_2 or filtered air) at a flow rate of 200 ml/s. Different heating protocols were used to produce heat-treated cotton with different properties. For heat treatment at 1000°C, the samples were produced using the following heating stages: room temperature to 150°C at 5°C/min in air followed by a thirty-minute isothermal period, 150°C to 250°C at 5°C/min in air followed by another thirty-minute isothermal process, 250°C to 600°C at 2.5°C/min in N_2, 600°C to 800°C at 1.5°C/min in N_2, and finally 800°C to 1000°C at 1°C/min in N_2 followed by a sixty-minute isothermal stage before naturally cooling down to room temperature. For heat treatment at 600°C or 800°C, the samples were heated to the target temperature following the same

13

protocol given above and was held isothermally for sixty minutes before cooling down. For the

heat-treatment at or below 210°C, the samples were directly heated to the final temperature from

room temperature at a rate of 5°C/min in either air or N_2 and held for sixty minutes isothermally.

Hydrothermal heat-treatment was carried out using an in-house built autoclave made of

stainless steel with an internal volume of 200 cm^3 and a sealed thermocouple located in the

center of the volume. A ratio of 2:1 distilled water to air was the chosen environment. The

autoclave was heated by an electrical heating jacket and the temperature was controlled by an

MCS SITC-15 temperature controller. Before heating, the autoclave was placed inside of a

secondary aluminum container to reduce temperature fluctuation. Each treatment involved

loading 133 ml of distilled water into the autoclave and gently placing a piece of cotton fabric (2

g) into the water until it was fully submersed. The autoclave was sealed and heated to the desired

temperatures at ~10°C/min. The temperature was maintained for sixty minutes before being

naturally cooled down to ~60°C. The treated fabric was removed from the autoclave and rinsed

repeatedly with distilled water until the water was clear without odor. The fabric was finally

dried in a vacuum oven at ~ 65°C for twelve hours. Trialing of the hydrothermal parameters

showed that the cotton materials degraded severely at temperatures above 210°C with an induced

pressure up to 1.4 MPa. Because of this, only autoclave treatments below 210°C were used in

this study.

Thermal treatment of cotton fabric has greatly varying effects which can be seen through

general observation. With increasing temperature there is a clear loss in total mass and surface

area of the samples as well as a gradual discoloration and degradation. *Figure 4* displays both

pristine cloth as well as cloths thermally treated in the furnace or autoclave under different

conditions. Below 200°C, gradual yellowing or browning of the samples with increasing

treatment temperature could be easily noticed for both treatment methods. Under high temperature environments (i.e., furnace treatment with N_2 at 600°C, 800°C, and 1000°C), the three samples showed nearly indistinguishable blackening, indicating high degree of carbonization. The three highly carbonized samples and the samples autoclaved higher than 180°C were fragile and needed to be handled carefully.
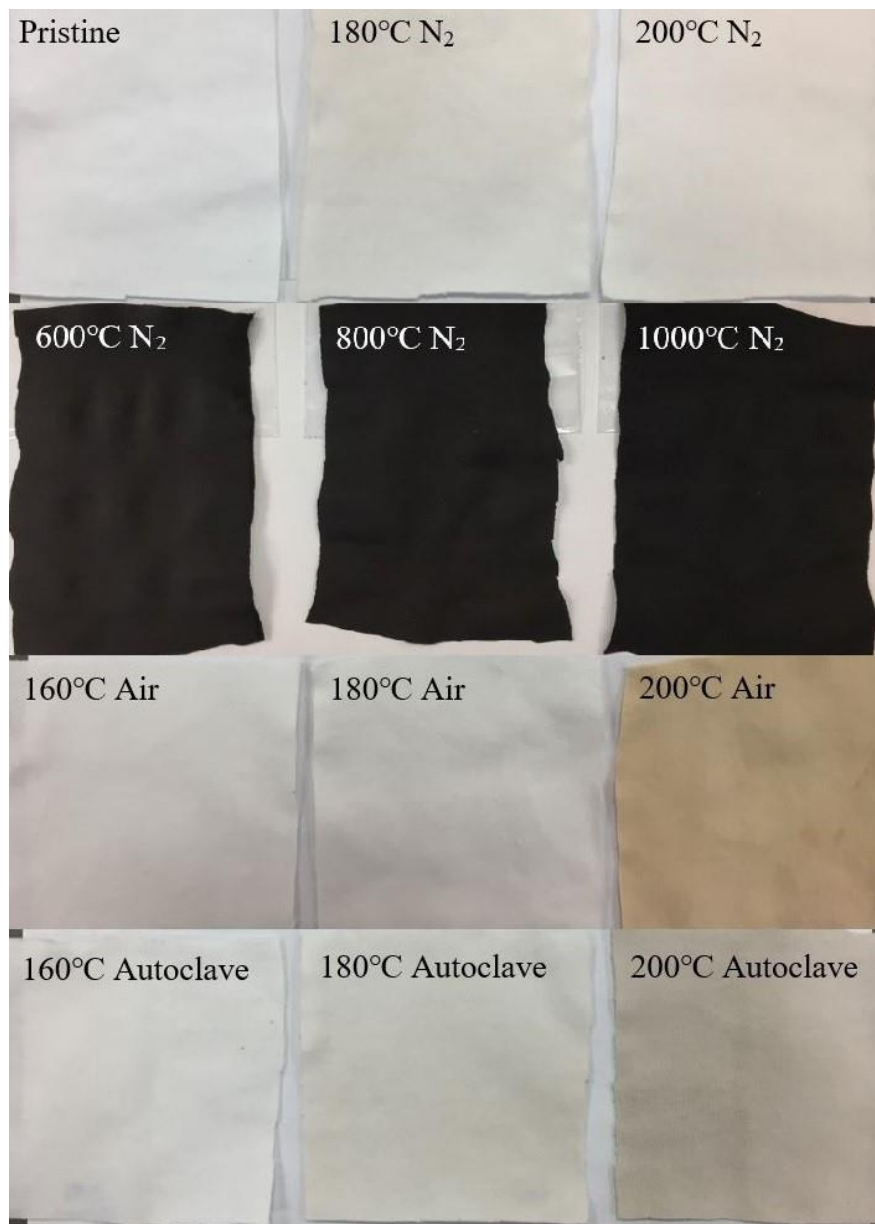
Figure 4. Cotton fabrics after heat treatment under varying conditions.

Composite Manufacturing

Composites were produced via a simple manual lay-up and compression molding method. First, thermally treated cotton fabric samples (100x100mm) were submerged in a bath of Clearcast 7000 resin and manipulated to ensure complete resin impregnation. Individual wetted samples were then placed side-by-side onto a release film on a level surface and immediately covered by a large steel plate wrapped in release film. Each composite manufactured contained a single layer of cotton fabric in the direction of the braid. Samples were let to rest under the steel plate for 24-hours before removal to ensure uniform compression and curing. Each sample was then let to rest an additional 12-hours in ambient air to ensure a full cure. Once fully cured, each single-layered composite sample was roughly 0.8mm thick and were cut into five 75mm by 12.5mm tensile testing bars using a wet jet tile cutter. Neat epoxy samples were made in a lay-up process as well alongside pristine cloth samples to ensure a similar thickness. Through weight ratio analysis of treated cotton fabrics before and after epoxy incorporation, rough fiber-epoxy weight fractions were found to between 18-22 wt% fiber and 82-78 wt% epoxy for low temperature treated samples and between 14-15 wt% fiber and 86-85 wt% epoxy for high temperature treated samples.

Characterization Techniques

Mechanical properties of the composites such as elastic modulus, ultimate stress, ultimate strain, and toughness were gathered from tensile samples made following the ASTM D3039-17 standard for polymer composite tensile testing. Neat epoxy samples were made to the same dimensions as the composites so that reasonable comparison could be displayed. To avoid damages to the tensile bars caused by griping, the grip area of the bars was reinforced by pieces of fiberglass reinforcement (25mm long, 3.25mm thick). Two were adhered to each side using

the same epoxy used for composite manufacturing as seen in *Figure 5*. Tensile testing was

conducted on an MTS Insight tensile apparatus at a rate of 60 mm/min until sample fracture.

Five repeats were conducted for each sample to get average tensile properties.
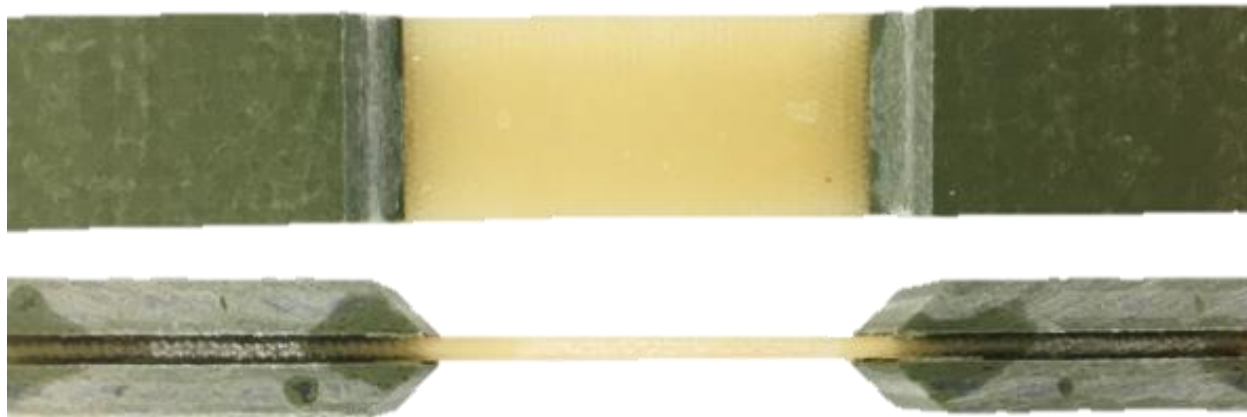
Figure 5. Cotton fiber and epoxy composite tensile bar.

Chemical bonding information of the treated cotton was studied using a Thermo

Scientific Nicolet 8700 FTIR operating under the ATR mode. The samples were scanned

between 4000 cm^{-1} and 625 cm^{-1} wavenumbers, and the spectra were obtained based on 32

repeated scans. Only samples treated at low temperatures (with a relatively low

degree of carbonization) were tested since samples treated above 600°C were too dark to be

analyzed due to their high carbon content absorbing most incident infrared light.

Scanning electron microscopy (SEM) was conducted to study the morphology of the

treated fabric using a JEOL JSM-6490LV at variable magnification. Samples were lightly coated

in carbon to increase conductivity for improved imaging. Fracture surfaces of the composites

obtained from the tensile testing were also imaged using SEM to study the fiber-epoxy interface

and the failure mechanism of the composites. Energy dispersive X-ray spectroscopy (EDS) was

also performed in tandem to analyze the elemental composition of the samples.

X-ray diffraction (XRD) was employed using a Bruker D8 Discover x-ray diffractometer to confirm the expected crystallographic structure with that of previous works and expectations. 12.5x12.5mm samples were fixed in the device via a glass slide and double-sided tape. Diffraction angles from 0° to 90° with a 15° step (2θ) were observed at 200sec per frame.

Thermo-gravimetric analysis (TGA) was carried out on a Perkins-Elmer Pyris 1 TGA using aluminum pans and stirrup. This technique provided a significantly more accurate understanding of the fabric dehydration compared to measurements from bulk samples produced. Before heating the samples, the furnace was sealed and purged with either air or N_2 for 10min. Heating proceeded by increasing the temperature from ambient to the desired temperature at 5°C/min before being held isothermally for sixty minutes.

Characterization Results

Tensile Testing

Samples tested varied from baseline neat epoxy and epoxy reinforced with pristine cotton fabric to a variety of epoxy reinforced with treated cotton fabrics as seen in *Figures 6 & 7* with data provided in *Tables 1 & 2*. Each sample showed unique results based on the form of treatment applied to the cotton fabric which signified that these treatment methods can alter the composite's overall strength. Comparing the neat epoxy to that of epoxy reinforced with pristine cotton fabric shows dramatic differences in all four properties measured. With the incorporation of cotton fabric, a near 11.8 times increase in elastic modulus and 3.3 times increase in ultimate stress were seen. In turn, ultimate strain and toughness are 23.4 and 7.4 times lower, respectively. This transition in properties is typical when comparing neat thermosets to their composite counterparts due to reinforcements restricting the flow of polymer chains and increasing overall rigidity.

Comparing the autoclave heat treated fabric epoxy samples to that of pristine fabric epoxy, it is clear that the autoclave treatment method can offer further improved elastic modulus, ultimate strain, and toughness while not degrading the ultimate stress. Little difference in properties though can be seen between the two lowest temperature autoclave treated samples (i.e., 140°C and 160°C) with only minor increases in elastic modulus and ultimate stress with increased temperature. As temperature of autoclave treatment continues to increase there is a distinct decrease in all but ultimate stress for 180°C while 200°C and 210°C show decreases in all properties likely caused by both elevated temperature and pressure. Autoclave heat treatment at temperatures above 160°C attributed to the degradation of the fabrics structure which was observed as frail and brittle samples in-hand.
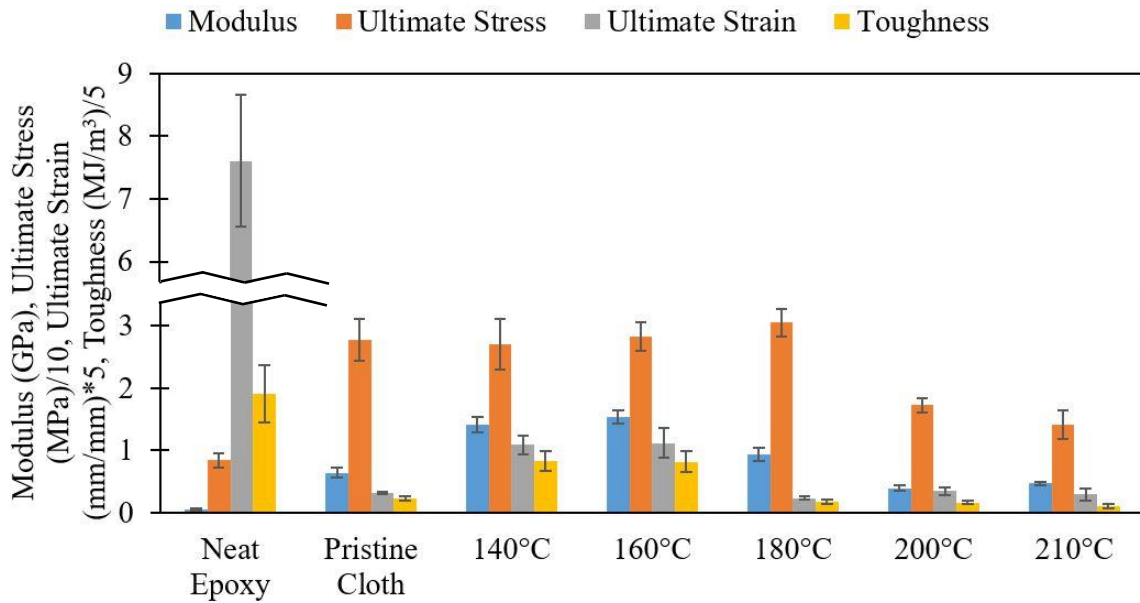
Figure 6. Tensile properties of neat epoxy, epoxy/pristine cotton composite, and epoxy/autoclave-treated cotton composites.

Table 1. Tensile properties of neat epoxy, epoxy/pristine cotton composite, and epoxy/autoclave-treated cotton composites.

Tensile Properties	Neat Epoxy	Pristine Fabric	140°C	160°C	180°C	200°C	210°C
Elastic Modulus (MPa)	54.8 ±15.8	643.9 ±84.4	1407 ±123	1541 ±112	940.3 ±109	396.5 ±44.8	470.4 ±34.7
Ultimate Stress (MPa)	8.4 ±1.13	27.8 ±3.38	27 ±4.07	28.3 ±2.28	30.5 ±2.26	17.3 ±1.14	14.2 ±2.29
Ultimate Strain (mm/mm)	1.522 ±0.211	0.065 ±0.004	0.218 ±0.031	0.224 ±0.048	0.0475 ±0.006	0.07 ±0.013	0.059 ±0.02
Toughness (MJ/m³)	8.55 ±2.27	1.15 ±0.205	4.14 ±0.81	4.11 ±0.833	0.87 ±0.175	0.83 ±0.143	0.55 ±0.2

Furnace heat-treated fabric at 160°C in air produced the largest increases in ultimate stress, ultimate strain, and toughness of all low temperature treated samples with a near 5 times and 5.8 times increase in ultimate strain and toughness respectively compared to pristine fabric reinforced epoxy. Elastic modulus is also seen to increase by a factor of nearly 3 with the largest increase seen in the 180°C treatment. Ultimate stress is also seen to increase slightly regardless of treatment temperature although there is no trend other than plateauing. A limit appears to be reached at treatment temperature between 140°C and 180°C which could be due to slight degradation of the fibers occurring at prolonged exposure to 180°C and higher temperatures. Interestingly, the ultimate stress is nearly unaffected in this temperature range which signifies that the treatment may not be strengthening the individual fibers but rather allowing them to dislocate farther without failure. Below 180°C in the inert nitrogen environment, nearly no changes can be visually seen on the samples and little property changes were found which is why only 180°C to 1000°C are displayed. Based on the data, the 180°C in N_2 provided the largest overall increase in ultimate stress compared to all other samples. While toughness is also increased in this sample, the elastic modulus and ultimate strain are seen to decrease compared to

pristine fabric reinforced epoxy. It is the lack of oxygen for the sample to react with in the nitrogen environment that causes a lower degree of effect compared to their air treated furnace counterparts.[40,41] Compared to the 200°C N_2 treated sample, trialing samples slightly above 200°C could display a similar set of properties and trends to that of the air heat-treated samples with an eventual plateauing or decreasing.

Higher temperatures, at and above 600°C, show promise for improvement likely due to the extreme degree of carbonization. Just like the air heat treated samples, the high-temperature samples displayed a gradual plateauing which signifies an optimal zone around 800°C. The reinforcing effect caused by these samples is quite different from the low temperature treated samples with dramatic improvement in allowable strain and toughness. However, the impact of such high temperatures caused the elastic modulus and ultimate stress to suffer leading to lower overall performance.

Even with the potential that arrives from the low-temperature autoclaved samples, furnace heat-treated samples seem to offer the most ideal reinforcing affects. This could mean different degrees of heat-treated samples can be sandwiched together for optimization of composites. Overall, the results show that the thermal treatment can be tailored for specific applications (e.g., if toughness is more critical than elastic modulus and so forth).
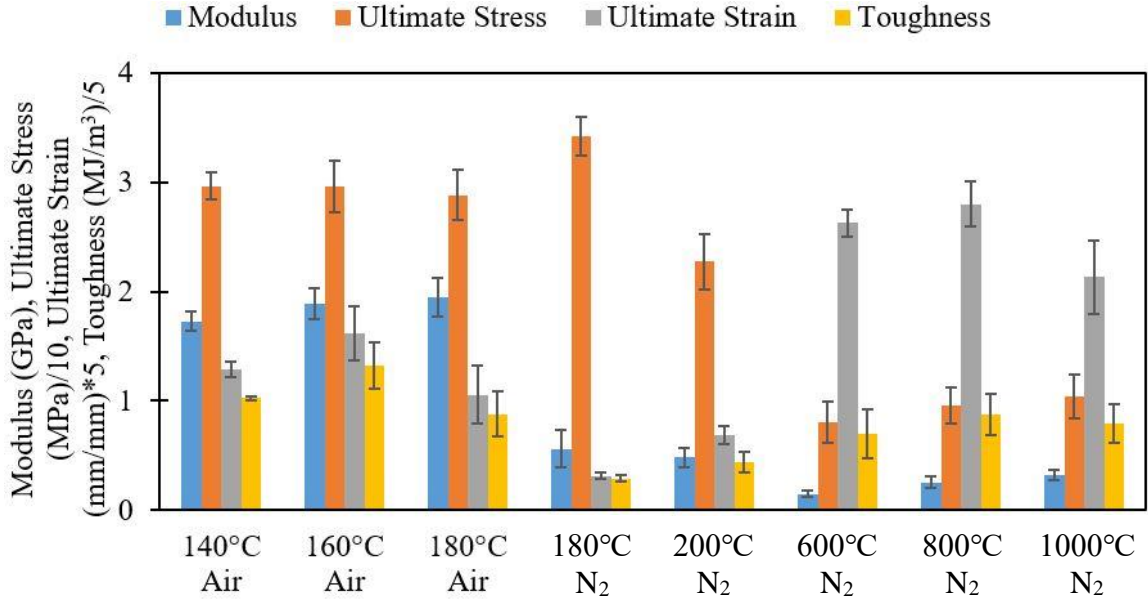
Figure 7. Tensile properties of epoxy/furnace-treated cotton composites.

Table 2. Tensile properties of epoxy/furnace-treated cotton composites.

Tensile Properties	140°C Air	160°C Air	180°C Air	180°C N_2	200°C N_2	600°C N_2	800°C N_2	1000°C N_2
Elastic Modulus (MPa)	1729 ±87.5	1891 ±143	1949 ±178	561.9 ±173	482.7 ±88.2	152 ±32.2	258.1 ±51.6	323.2 ±49.1
Ultimate Stress (MPa)	29.6 ±1.27	29.6 ±2.36	28.8 ±2.28	34.2 ±1.76	22.8 ±2.53	8.1 ±1.87	9.6 ±1.69	10.4 ±2.01
Ultimate Strain (mm/mm)	0.258 ±0.015	0.323 ±0.05	0.212 ±0.052	0.06 ±0.006	0.138 ±0.017	0.525 ±0.013	0.56 ±0.021	0.426 ±0.034
Toughness (MJ/m³)	5.13 ±0.093	6.62 ±1.07	4.39 ±1.04	1.42 ±0.145	2.21 ±0.451	3.5 ±0.226	4.4 ±0.188	3.97 ±0.174

Thermo-Gravimetric Analysis

Weight loss of the fabric after the treatments are summarized in *Table 3* and displayed in *Figure 8*. In both air and N_2 environments, the weight loss of the furnace-treated samples increased with increasing temperature. Dehydration is assumed to be the main weight loss mechanism during cellulose pyrolysis when the temperature is low. It was clear that the samples treated in air exhibited higher weight losses than those treated in N_2 under the same temperatures

(i.e., 180°C and 200°C), likely due to the inert nature of N_2 inhibiting the small degree of oxidation occurring at the low temperatures. Sample weight losses at 600, 800, and 1000°C are close, suggesting a similar degree of carbonization under these three temperatures. With a 1.1% difference between 600°C and 800°C, but only a 0.1% difference between 800°C and 1000°C, it can be assumed that 800°C is roughly the maximum temperature needed for complete carbonization.

Hydrothermal carbonization of cotton produces carbon-rich solid residual (i.e., biochar) and soluble organic substances under low temperatures (< 300°C). The process mainly includes cellulose hydrolysis, cellulose depolymerization into soluble substances (e.g., glucose and oligomers), and polycondensation/polymerization of some solubles. Cotton fiber loses mechanical strength and fragments relatively quickly (< 2 hours) during the process, with a higher temperature leading to faster and more severe disintegration. The weight losses for the hydrothermally treated samples given in *Table 3* is primarily due to cellulose hydrolysis and depolymerization. Since the TGA cannot perform hydrothermal treatment, weights were obtained by weighting the samples on a standard scale after drying. The losses increased with the increasing temperature; when the temperature was higher than 200°C, the fabric was too fragile to be handled in composite fabrication.
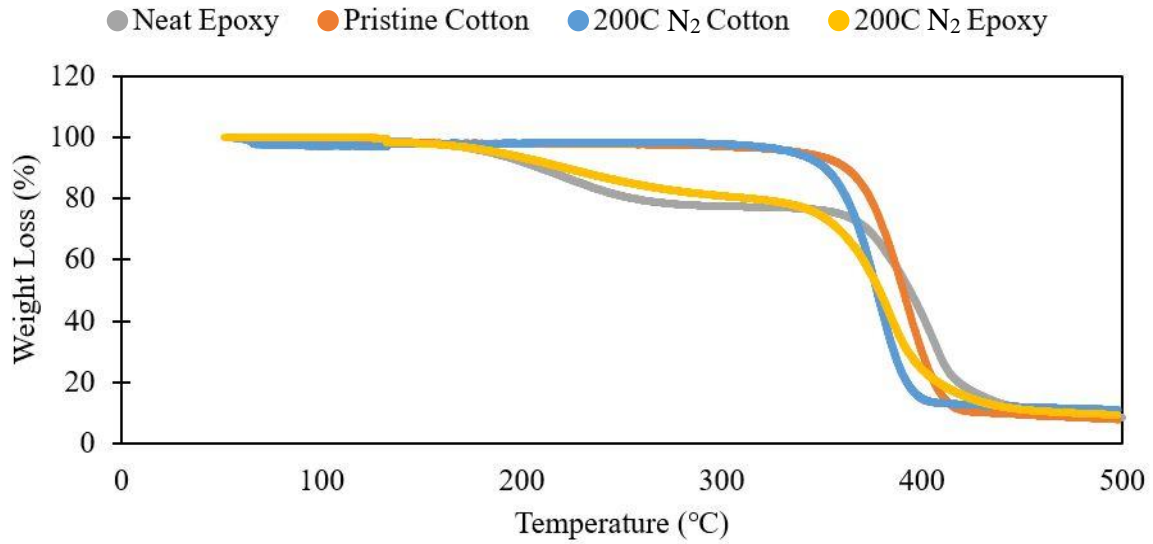
Figure 8. Percent weight loss of neat and treated fabrics and composites.

Table 3. Mass loss after various heat-treatment.

Thermal Treatment Method	Temperature/ Environment	Weight loss (%)
	140°C Air	2.98
	160°C Air	4.48
	180°C Air	4.68
	200°C Air	5.35
Tube Furnace	180°C N_2	3.15
	200°C N_2	3.26
	600°C N_2	82.4
	800°C N_2	83.5
	1000°C N_2	83.6
	140°C	2.43
	160°C	3.12
Autoclave	180°C	3.88
	200°C	5.31
	210°C	11.18

Fourier-Transform Infrared Spectroscopy

Comparing pristine cotton to autoclave cotton in *Figure 9*, three new peaks at 1745 cm^{-1} (C=O), 1645 cm^{-1} (C=C), and 1590 cm^{-1} (conjugation of C=O or C=O with aromatic structure) appear, and the peak at 1634 cm^{-1} disappears. The intensity of the new peaks fluctuate with increasing treatment temperature, showing the highest overall peak in the 160°C air sample. This can be explained as physical desorption of water (25-150°C) from the hydroxyl groups in the cellulosic units (150-240°C).[40,42] The dehydration reaction can also be confirmed by decreased peak intensity of O-H (3000-3690 cm^{-1}), C-O (1106 cm^{-1}), and C-OH (1055 cm^{-1}) groups at higher treatment temperatures.[42] Therefore, the dehydration reaction rather than the decarboxylation reaction occurs under this temperature region when using the tube furnace. This would explain the difference in properties between the low and high temperature tube furnace heat-treated samples since at low temperatures only dehydration is occurring while at high temperatures both dehydration and decarboxylation are occurring. Comparing the spectra of the sample treated at 140°C in the autoclave with the sample treated at 140°C in air in the furnace, as well as the sample treated at 180°C N$_2$ with the sample treated at 180°C air in furnace, it is seen that high pressure and air atmosphere are more beneficial for the dehydration process, leading to products with a greater number of oxygen-containing functional groups. These functional groups could explain the increase in properties as improved adhesion between polymer and reinforcements are known to improve with the introduction of surface functional groups for bonding. While functional groups can assist in interfacial adhesion, physical topography of the fibers also plays a significant role which is why SEM scanning is employed for observation.
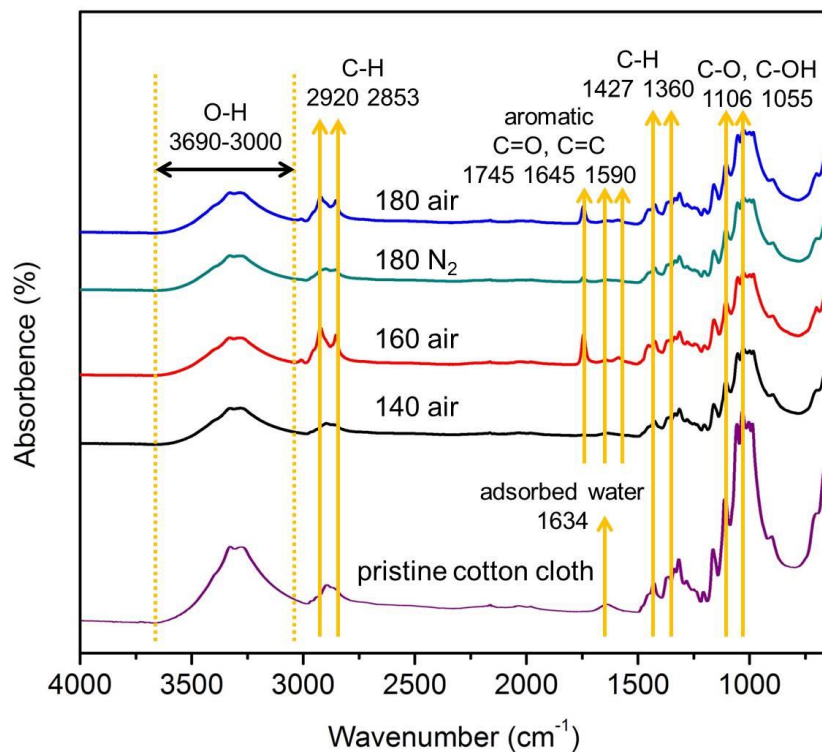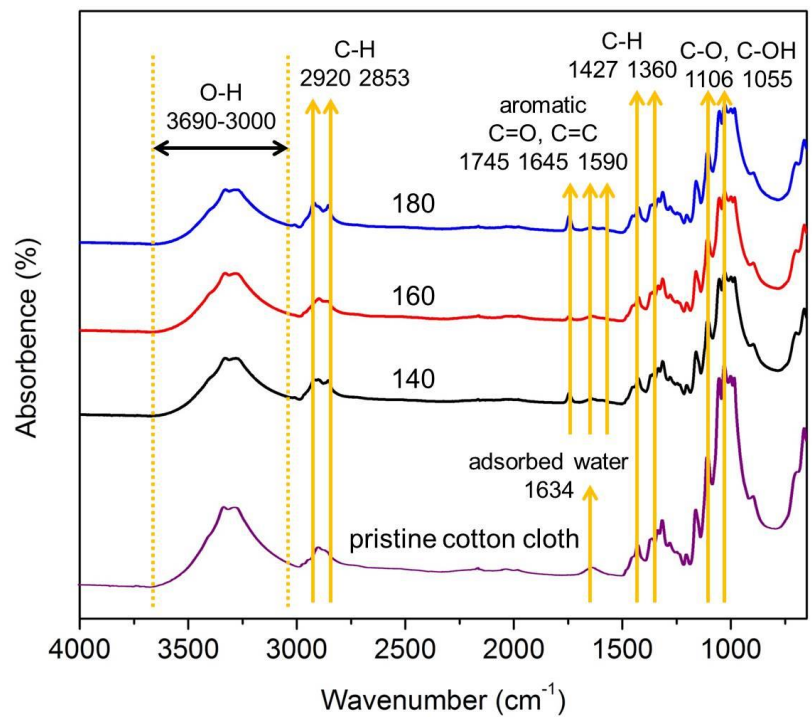
Figure 9. FTIR spectra of pristine cotton cloth and the derived products treated with autoclave (top) and furnace (bottom) methods under different temperatures.

Scanning Electron Microscopy

SEM imaging was done on neat epoxy, pristine cotton, and a variety of treated cotton cloth as well as their composite counterparts at both x500 and x5000 magnification as seen in *Figure 10*. Examining pristine cotton fiber, the iconic twisted and slightly wrinkled structure can be seen to form a sort of collapsed tube. Comparing each treated cotton cloth sample to the pristine fibers, it is immediately seen that the cloth heat-treated at 180°C in nitrogen has very little surface structure difference except for slightly more prominent wrinkling. Helical wrinkling has been shown to occur on heat treated cotton fibers in previous works and is known to show the direction of the cellulose strands.[15] This along with the minimal weight change suggests negligible physical or chemical alterations and could corroborate the similarities in mechanical properties between the pristine cotton and 180°C nitrogen samples.

Viewing the autoclaved fibers also shows a similar surface structure to that of pristine fibers yet with deep wrinkles and loose cellulose strands littering the surface suggesting both densification and degradation. Loose cellulose strands are likely a result of amorphous cellulose degradation since crystalline cellulose has a larger hydrophobicity. These features increase the effective surface area of each fiber to potentially allow for improved adhesion in a polymer matrix. This slight yet noticeable change in surface structure helps to explain why the 180°C autoclave sample is only marginally better than the pristine cloth sample but can show an improved modulus compared to the 180°C nitrogen sample.

A dramatic difference is seen between the pristine fibers and the 180°C air fibers where severe wrinkling and depressions litter the surface of the latter. Unlike in the other low temperature treated fibers, 180°C air fibers have more irregular wrinkling outside of the natural cellulose direction. These changes are likely an effect of extreme dehydration occurring in the air

environment which is known to cause the inner layers of the cottons tubular structure to shrink and conform around one another.[15] With the dramatically increased surface roughness, it could be expected that a better bonding in the composite matrix can be obtained which leads to improved properties as seen in the tensile test.

Moreover, the air heat-treated sample has the smallest average diameter among all the low temperature treated fibers at just 16.5µm, which gives these fibers the largest aspect ratio (assuming the average fiber lengths of each sample are equivalent) and therefore the strongest interfacial bonding between the fibers and the epoxy matrix. The small diameter of the air heat-treated fiber also suggests that the fiber was densified to the highest relative degree of the low temperature treated fibers which could also attribute to the highest overall toughness. Other average diameters include 18.6µm for the pristine cotton, 17.3µm for the autoclaved heat-treated cotton, and 16.7µm for the nitrogen heat-treated cotton. A major difference can be seen in the 600°C and 1000°C cotton where average diameters were found to be 10.1µm and 9.8µm, respectively. While there is very little weight loss difference between the two high temperature treated fibers, the 0.3µm difference suggests that increasingly elevated temperatures can further densify the fibers. From this information, it is clear that the physical structure of the cotton fiber is dramatically altered via the thermal treatment processes and is likely being mechanically improved due to the topography changes.
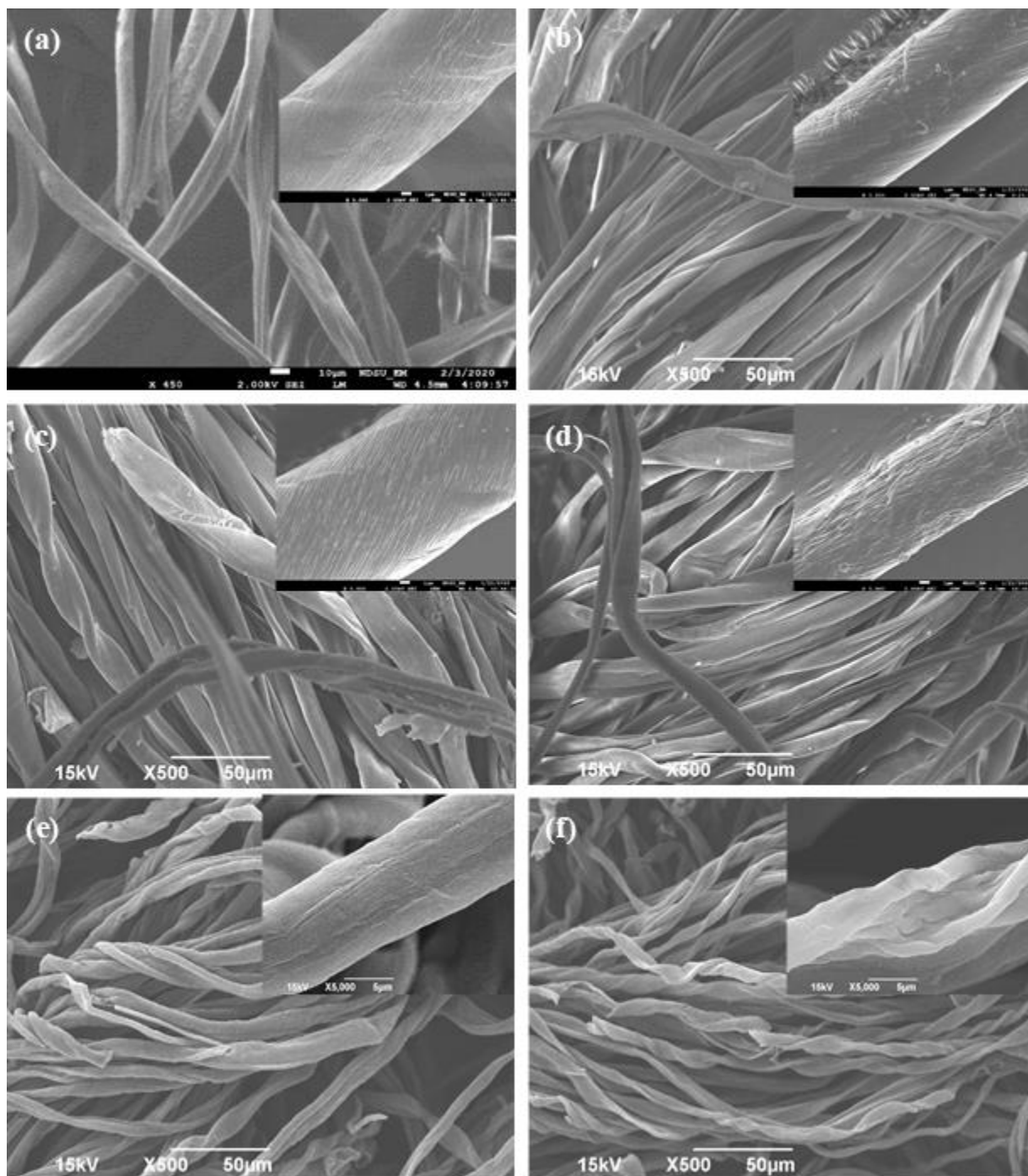
Figure 10. SEM images of the cotton in pristine condition and after different thermal treatments: (a) pristine, (b) 180°C/autoclaved, (c) 180°C/N$_2$, (d) 180°C/air, (e) 600°C/N$_2$, and (f) 1000°C/N$_2$ at 500 and 5000 magnifications.

Fracture surfaces of tensile samples were gathered to study the bonding at the fiber/epoxy interface and the distribution of fibers in the epoxy as seen in *Figures 11 & 12*. Neat epoxy expectedly has a smooth fracture surface and a uniform internal structure with some minor imperfections near the air-epoxy interface. Examining the differences between the fiber composites, distinctive gaps at the epoxy-fiber interface are seen in the pristine and both autoclaved samples. These gaps could be caused by weak bonding to the fiber which also attribute to the minor fiber dislocation or pull-out as seen. A key difference though is that the autoclaved samples display significant peeling on their surface which may be attributed to degradation or weakening of the fibers outside layer. A weak fiber layer at the interface with epoxy would justify the similar if not lower properties seen in autoclaved samples versus pristine which has no such degradation. Examining the 160°C air sample shows a significantly improved interfacial adhesion over the pristine cloth with less fiber dislocation and small to no gaps. While some gaps are still present, there is no sign of fiber surface degradation which would assist in halting dislocation and improving mechanical properties. In contrary to all other samples, the 800°C N_2 sample displays near ideal interfacial adhesion with no gaps and little dislocation. While this would explain the significantly improved properties in comparison the pristine cotton, the drastic difference between low and high temperature furnace treated samples could be due to the high-temperature fibers smaller fiber diameter leading to a larger surface area per volume.
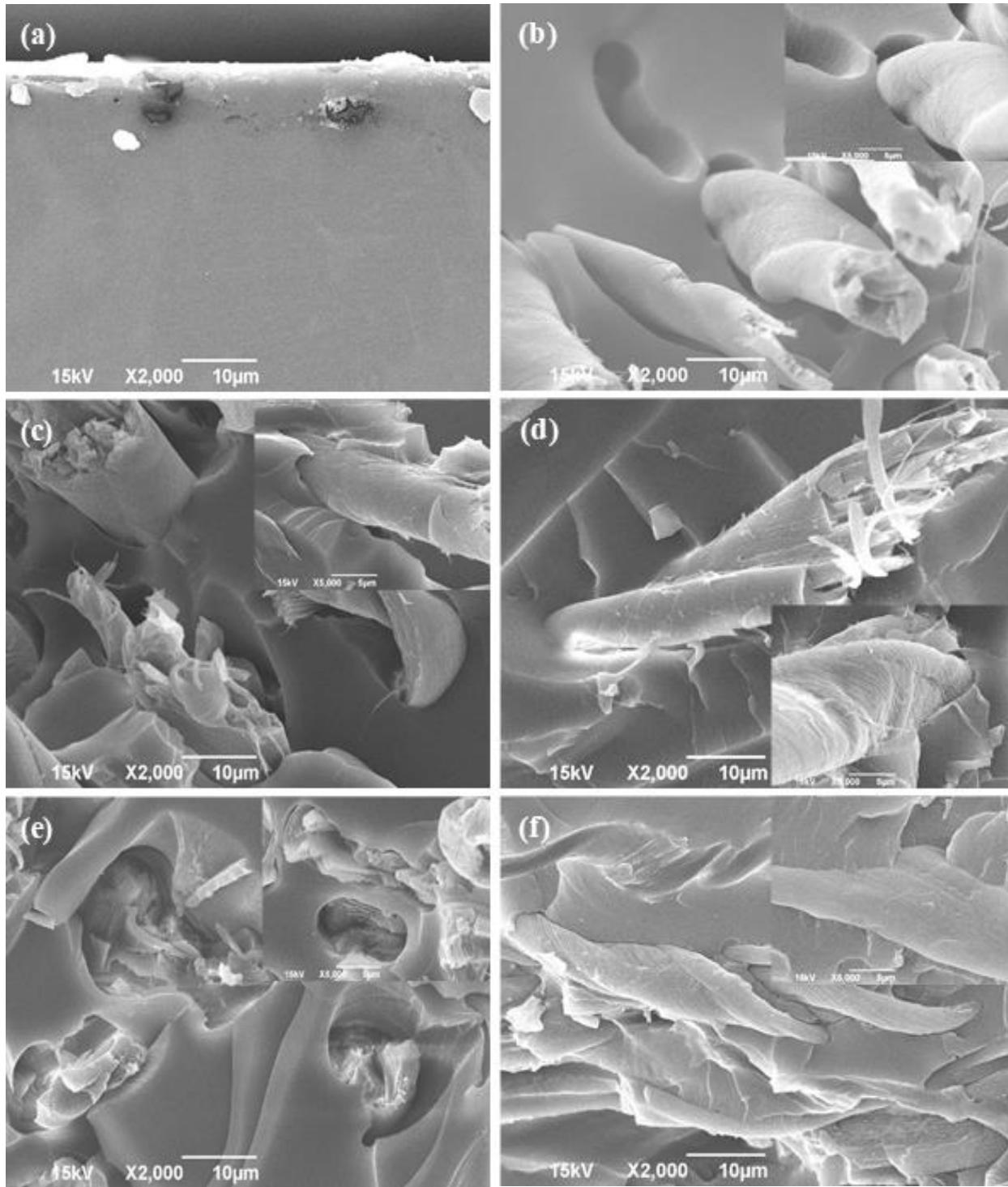
Figure 11. SEM images of the fracture surfaces of neat epoxy (a) and the composites reinforced with pristine cotton (b) and treated cotton: 160°C/air (c), 160°C/autoclave (d), 200°C/autoclaved (e), and 800°C/N_2 (f) at 2000 and 5000 magnifications.
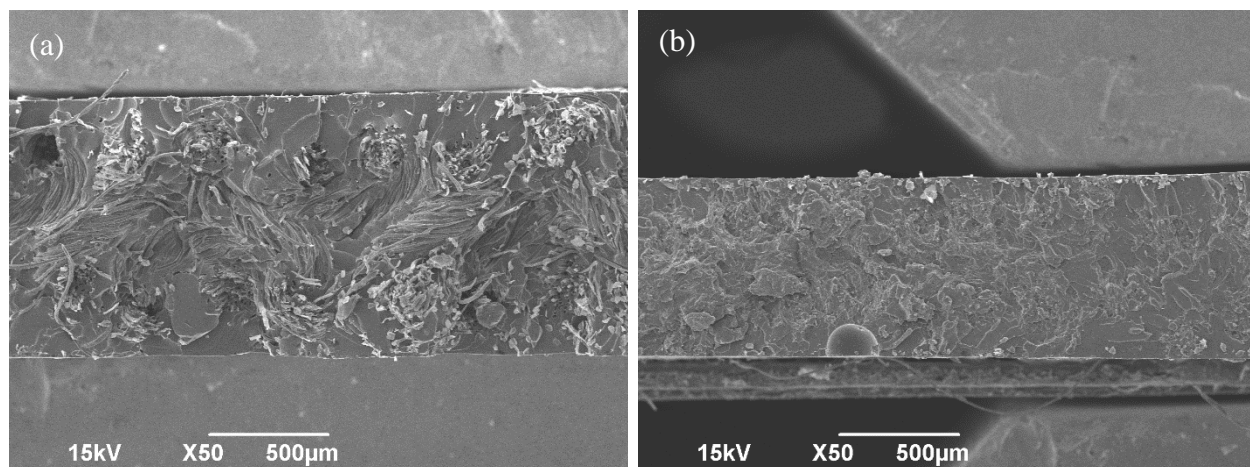
Figure 12. SEM images of the fracture surfaces of epoxy/cotton composites containing pristine cotton (a) and the 800°C/N_2 cotton (b) at 50 magnification.

Electron Dispersion X-Ray Spectroscopy

Elemental analysis was conducted on 180°C samples as well as pristine fiber. Five points were sampled on each fiber to get an average elemental composition. As shown in *Figure 13* and *Table 4,* all four samples exhibit very similar carbon and oxygen contents, suggesting the composition of the fibers are not dramatically different. While the carbon coating does have influence on the carbon percentage for each sample, the relative differences remain since each sample was coated simultaneously. The trace amount of aluminum in the samples is likely due to the decomposition of the alumina boats used in sample production. Results for pristine cotton are comparable to those found of cotton and cellulose is previous studies.[43,44] This reinforces the theory offered by FTIR that dehydration rather than carbonization is occurring in the low-temperature treated samples. Comparing each sample shows a subtle but definite trend in degree of carbonization depending on the manufacturing method. An air environment appears to offer the highest degree of heat-treatment which is expected since nitrogen is an inert gas. While the air and autoclave heat-treated samples have the nearest values, it is possible that the enclosed

nature of the autoclave compared to the flowing gas in the furnace reduces the allowable

carbonization.
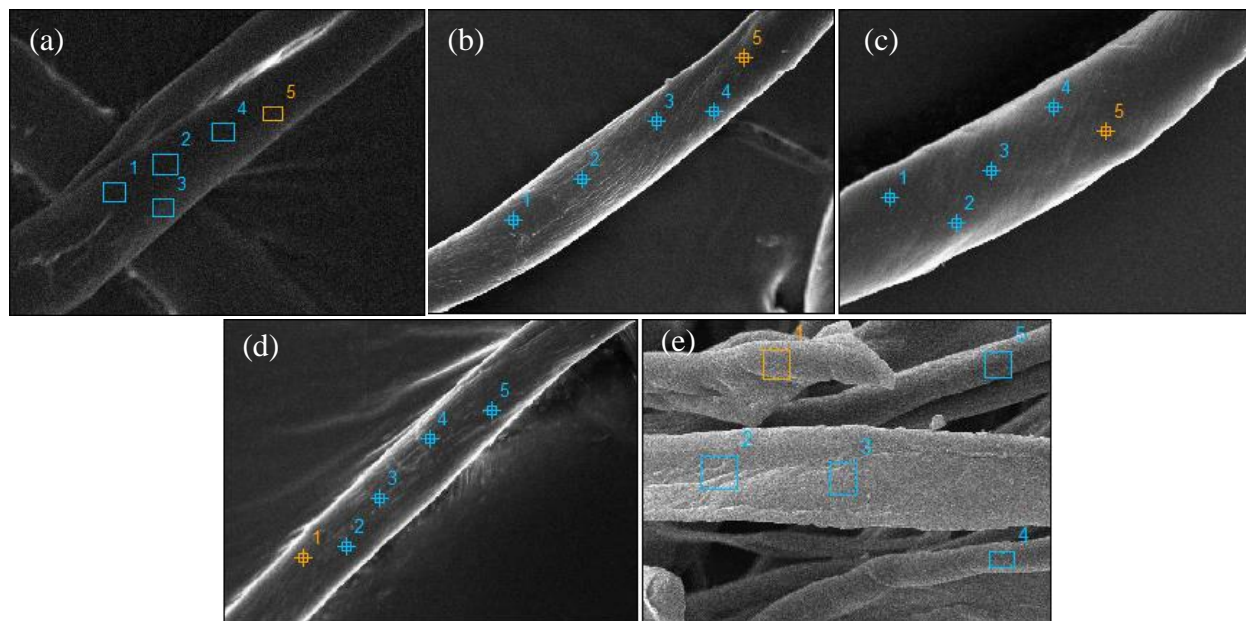
Figure 13. Elemental analysis of the pristine and thermally treated cotton through EDS on five locations of each fiber: (a) pristine, (b) 180°C/air, (c) 180°C/N_2, (d) 180°C/autoclave, and (e) 600°C/N_2.

Table 4. Average atomic composition for pristine and differently heat-treated cotton cloths.

Sample	Carbon (%)	Oxygen (%)	Aluminum (%)
Pristine Cotton	53.46	46.54	0
180°C/N_2	53.79	45.91	0.30
180°C/Autoclave	54.49	45.17	0.34
180°C/Air	54.87	44.80	0.33
600°C/N_2	99.77	0	0.23

X-Ray Diffraction

X-ray diffraction was performed on both pristine and 600°C treated cotton fabric to

further confirm the carbonization of cellulose. *Figure 14* shows the 2D diffraction patterns of the

two samples while *Figure 15* presents their diffraction spectra extracted from the patterns.

Pristine cotton exhibited characteristic peaks at 14.98, 16.7, 22.63, and 34.49° representing the

101, 10$\underline{1}$, 002, and 040 crystallographic reflections, respectively, of cellulose I as seen in *Figure 14*. These peaks disappeared from the cotton treated at 600°C and presumably higher temperatures, indicating complete destruction of the cellulose's crystallinity after the treatment. This can be interpreted from the peaks at 7.74 and 18.45° on the treated sample which are broad with poor definition indicating a lack of crystallinity and a generally amorphous structure. Similarities in peaks can be seen between this carbonized cotton and amorphous carbon powders.
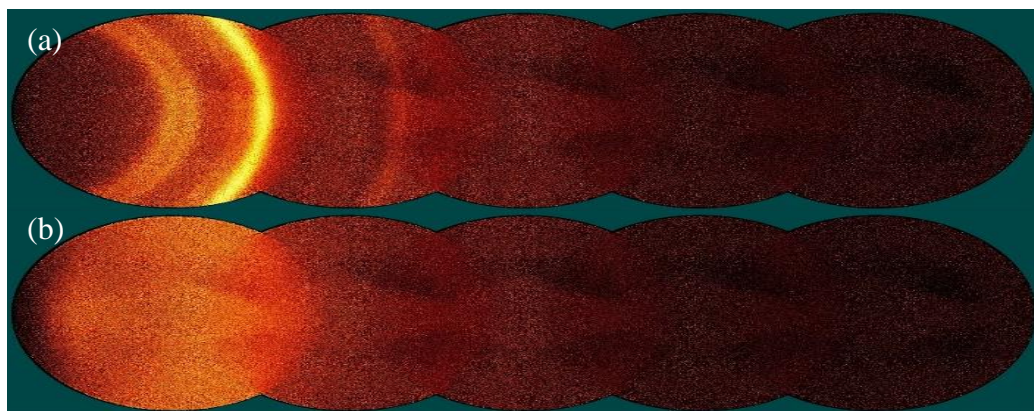
Figure 14. 2D X-ray diffraction pattern of (a) pristine and (b) 600°C treated cotton fabrics.
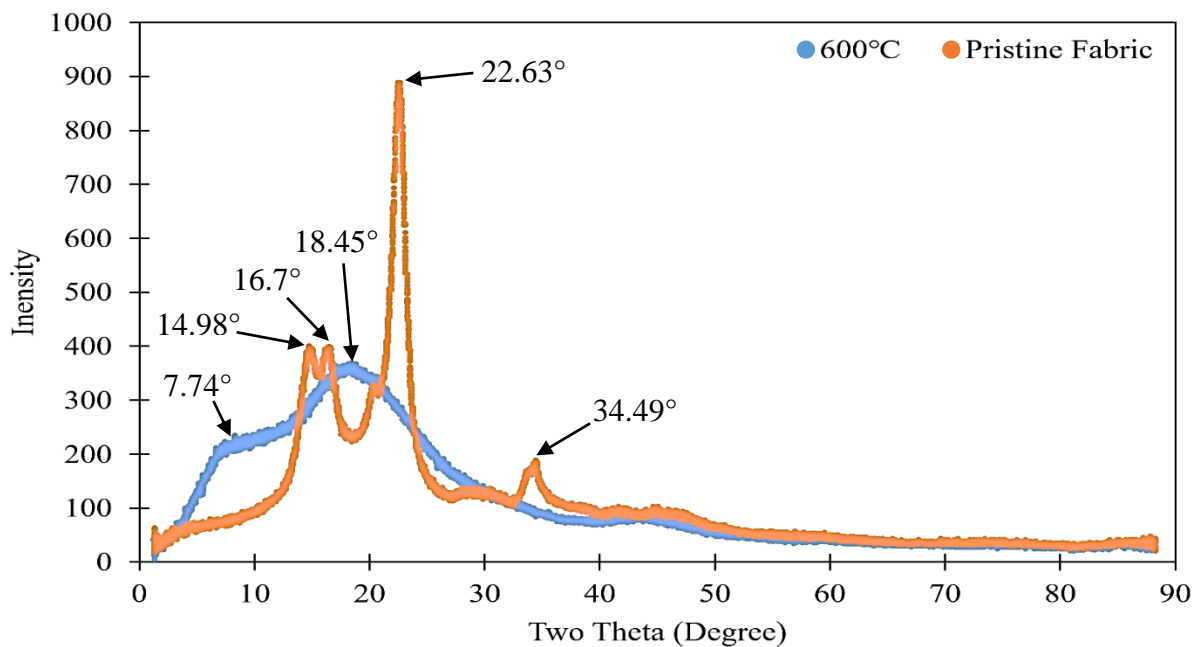
Figure 15. X-ray diffraction spectra of pristine and 600°C/N$_2$ treated cotton fabric.

Discussion

Being that the walls of the cotton structure have increasing cellulose crystallinity towards the center of their form, the outer most wall was relatively low crystallinity at around 30%. Significantly more amorphous cellulose on the outer wall will undergo hydrolysis initially during hydrothermal treatment which forms glucose oligomers and monomers weakly bonded to the crystalline walls.[23] Weakly bonded glucose formations have been found at treatments as low as 100°C, but separation into glucose molecules doesn't occur until 150°C for the amorphous region and up to 180°C for the crystalline.[23] As the crystalline region begins to succumb, it transitions into an amorphous phase before decomposition.[24] These findings correlate well to the loss in properties seen in *Figure 6* for samples autoclaved at and above 180°C, justifying that autoclave treatments that degrade the crystalline region are detrimental.

Besides glucose, fructose is also formed during hydrolysis which rapidly undergoes dehydration into hydroxymethylfurfural (HMF).[7,45] Formation of HMF from cellulose has been characterized by decarboxylation and dehydration causing the increased C=O and decreased O-H stretching respectively. Correlation can be seen to *Figure 9* where the FTIR spectra reflects similar fluctuation. Further confirmation is seen with decreasing C-O and moderately defining C-H and C=C stretching intensities.

At temperatures under 220°C, oxidation and dehydration are found to be the two prominent mechanisms for the degradation and yellowing of cellulose materials.[40,42] Oxidation can occur in a variety of ways using oxidating chemicals (e.i., O_2), light/irradiation, or heat. However, each have the effect of converting -OH groups into C=O and COOH which are responsible for the chromophore yellowing and hastening the effect respectively.[41] Dehydration typically occurs when using light/irradiation or heat on cellulose which removes physically

absorbed water at low temperatures while at high temperatures cause -OH groups to react and produce C=O and unsaturated bonds along the pyranose ring (C=C).[42] These effects correlate to both the observed physical yellowing of low temperature treated samples in *Figure 4* as well as the emerging peaks seen on the FTIR spectra in *Figure 9*. Oxidation and dehydration are both confirmed in the tube furnace treated samples with FTIR peaks representing C=O and C=C developing. As expected, this correlated to the decrease in O-H and C-H peak intensities as -OH groups are converting. Further understood from *Figure 9* is that furnace treated samples below 140°C/air or below 180°C/N$_2$ have very gradual chemical alteration occurring signified by the minimal increase in C-H, C=C, and C=O bond stretching.

Further affirmation of the individual cellulose wall degradation is displayed through the morphology studies. Autoclaved treated fabric displayed increased fragility at temperatures above 180°C with *Figure 10b* displaying the premature signs of crystalline cellulose degradation. Fabrics autoclaved under lower temperatures at 140°C and 160°C could be expected to have an increase in mechanical properties due to the degradation of more amorphous walls leading to a stronger overall fiber.[24] This explains the distribution of mechanical properties for autoclaved cotton fabrics in *Figure 6* with moderate improvements in each composite up until 180°C.

Treatment of cotton fabric via tube furnace had considerably different results due to the gas environment. Morphology showed minor alterations occurring to the 180°C/N$_2$ treated fabric which was the nearest atomistic equivalent in *Table 4* to pristine cotton and visibly appears to have little topographical differences between *Figures 9a & 9c*. On top of it only having a 3.15% weight loss, the FTIR study showed miniscule intensities of C-H, C=O, and C=C bond stretching. Subsequently, the mechanical properties in *Figure 7* reflect these findings with only minor improvements to ultimate stress and toughness. Furnace treatment at 180°C/air however

showed tremendous improvement in mechanical properties with observations showing increased

yellowing, weight loss, and FTIR peak intensities attributed to the oxidation and dehydration

reactions. Comparisons agree with other studies which attribute the higher dehydration in air

treated samples compared to N_2 to the formations of hydroperoxide groups and subsequent

hydroxyl radical in the cellulose of the air environment which formed water through hydrogen

abstraction.[46,47] Based on these results, thermal treatment in air will provide the quickest

improvement due to the tandem oxidating and dehydration effects compared to the sole

dehydration affect in an N_2 environment

Increases in mechanical properties are seen not just at 180°C/air, but also at the

preliminary 140°C/air and 160°C/air conditions with the 160°C/air displaying the greatest. These

improvements can be attributed to factors a such as improved interfacial adhesion between the

fibers and epoxy as well as interfacial friction. Results from FTIR in *Figure 9* display the

reduction in polar -OH groups and the increase in less polar C=O and nonpolar C=C bonds

which alter the cottons natural hydrophilicity to a more hydrophobic nature. Surface roughness is

clear in *Figure 10d* the dehydration reaction removes physically absorbed water which densifies

the fiber and wrinkles the surface. These factors are confirmed with visually improved interfacial

and decreased fiber pullout on the fracture surface SEM micrographs. Combined, these factors

promote the transfer of stress from the matrix to the fiber so that the fiber can utilize its strength

potential.

Temperatures at and above 600°C/N_2 undergo a spectrum of reactions including

polycondensation, dehydrogenation, and deoxidation of char which culminates into a highly

carbonized fabric nearly a tenth of its original weight.[48] This attributes to the shriveled and

jagged fibers seen through SEM in *Figures 10e & 10f*. Results from EDS in *Table 4* confirm that

only carbon remains in the structures of high temperature treated cotton fibers. Carbon structures are normally mechanically strong, however XRD proves that the entirety of carbon in their structure is amorphous. Amorphous carbon is known to have minimal strength properties which justifies the low mechanical properties for high temperature treated fibers observed in *Figure 7*. Increase in ultimate strain is likely attributed to extreme interfacial bonding expected of pure carbon structures. This proves that thermal treatments above 600°C will likely be more detrimental than helpful for cellulose products as composite reinforcement.

Conclusion

Thermal treatment of cotton fabric was explored via furnace and autoclave in variable gas and temperature environments for incorporation into epoxy composites. Promising results were found with tremendous variance depending on treatment showing clear potential for tailored properties. Autoclave treatments saw initial improvements attributed to amorphous cellulose removal, however above 180°C the crystalline cellulose began to degrade causing dramatic weakening. Furnace treatments surpassed autoclave's viability with both low and high temperature treatments possible up to 1000°C. Treatment above 600°C however fully carbonizes the cotton fabric as seen in EDS and offers little strength as composite reinforcement due to its amorphous structure determined in XRD. Low temperature furnace treatments prevailed by increasing most mechanical properties both in air and N_2 environments. These improvements are attributed to increased surface friction caused by dehydration seen via SEM and FTIR, however air treatments also experienced oxidation which further improved their properties by creating increased hydrophobicity through the destruction of polar for less or nonpolar bonds. From this analysis, low temperature thermal treatment with a furnace in an air environment can be said to offer the most improvement in interfacial adhesion for epoxy composites. Applications for these

composites are countless with potential as reinforcement in skateboards, helmets, or even automobile parts due to both its affordability and its customizability through variable treatment. Culminated from these findings is proof of the environmentally friendly alternative to traditional interfacial adhesion improvement methods of cotton composites using thermal treatments.

ACRYLATED EPOXIDIZED COTTONSEED OIL AS 3D PRINTABLE RESIN

Introduction

Crosslinkable natural oil-based resin is not uncommon in the market with acrylated epoxidized soybean oil (AESO) being the most common natural oil used for this purpose. In this chapter, acrylated epoxidized cottonseed oil (AECO) and dimethacrylated epoxidized cottonseed oil (DMECO) were trialed to study both their mechanical properties as well as their potential viability as 3D printable resin.

By combining the AECO with a type I free radical photo-initiator, the resin can be cured under mild UV excitation which makes it practical for current methods of SLA 3D printing. AECO alone is notably more viscous than typical resins used for coatings and 3D printing which is why lower viscosity reactive diluents were added in various quantities. Since reactive diluents can be crosslinked and each have unique chemical structures, they provide unique properties to the resins, making it necessary to sample several oil and diluents combinations. While the diluents lower the resin's viscosity, they also help form a stronger crosslinked network improving mechanical properties. Diluent quantities varied from 0 wt% to 50 wt% since at 0 wt% SLA printing is impossible due to the high viscosity of AECO.

Tensile testing as well as DMA were employed to characterize the mechanical properties of each formulation. Through these methods a variety of properties were obtained including elastic modulus, ultimate stress, ultimate strain, toughness, and glass transition temperature. Based on the properties, specific formulations were trialed in an SLA 3D printer to test the overall printability of each as well as to compare potential viable and unviable structures. Also explored were the effects of varying (gas environment and temperature) post-curing treatments on the final products. Incorporation of thermal initiator into the 3D printed parts allowed for both

UV and thermal post-curing techniques to be compared as well. In summary, a comprehensive examination of AECO's potential as a 3D printable resin is conducted.

Formulation Preparation

Resin Formulations

CSO based resin formulations consisted of either AECO or DMECO, which were synthesized by Dr. Dean Webster's group at NDSU. AESO as well as the photo and thermal initiators, Omnirad TPO-L and Luperox P respectively, were purchased from Sigma-Aldrich. Clear differences in functionality are seen in *Figure 16* with AECO only having on average three unsaturated C=C bonds compared to AESO's five which can be reacted to form hydroxide and acrylic groups. Also purchased from Sigma-Aldrich were the diluents including tripropylene glycol diacrylate (TPGDA), trimethylolpropane triacrylate (TMPTA), pentaerythritol tetraacrylate (PETA), and 1,6-hexanediol diacrylate (HDDA) displayed in *Figure 17*. Each diluent molecule comprised of at least two acrylate groups which act as reactive sites for crosslinking under the activation by free radicals. Differences such as the ethyl- group in TMPTA, long molecule chain in TGPA, four acrylic groups in PETA, and short chain in HDDA will each have various effects on the resin's mechanical properties.
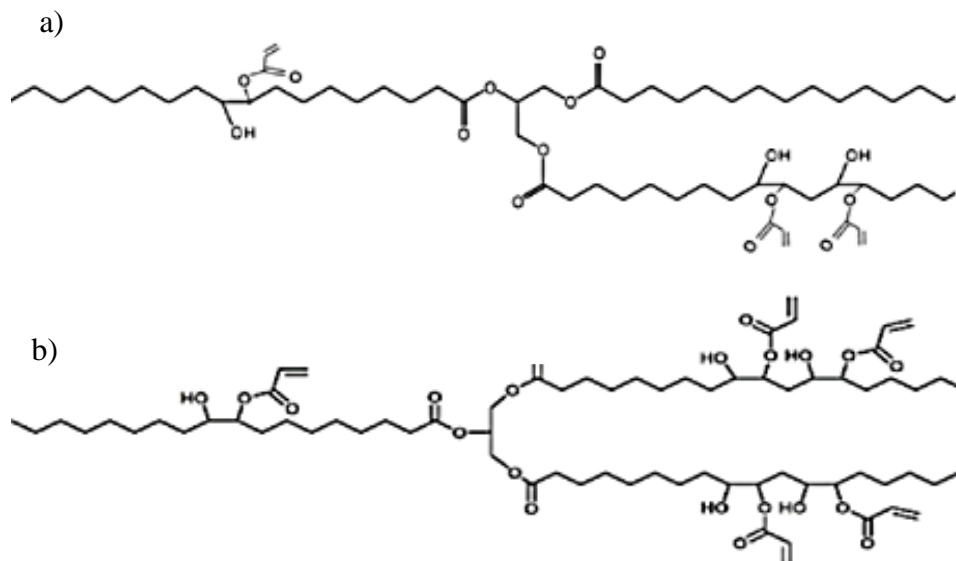
Figure 16. Representative molecular structure of a) AECO and b) AESO.

Synthesis of each modified oil was conducted by Dr. Dean Webster's group through a two-stage process including epoxidation and acrylation as seen in *Figure 3*. Briefly, epoxidation required amberlite and acetic acid to be added to the oil at an elevated temperature and mixed for up to seven hours. Hydrogen peroxide was gradually added to control generation of peracetic acid. Acrylation required acrylic acid as well as catalyst to be mixed with the ECO at an elevated temperature for up to twenty-four hours with the addition of an inhibitor once a specific acid value was obtained. Dimethacrylation required both methacrylic acid and methacrylic anhydride along with a catalyst and inhibitor to be mixed with ECO. Mixing at an elevated temperature with the catalyst, acid, and ECO proceeded until the acid was mostly reacted; at which point the anhydride was added and reacted until a specific acid value was obtained.
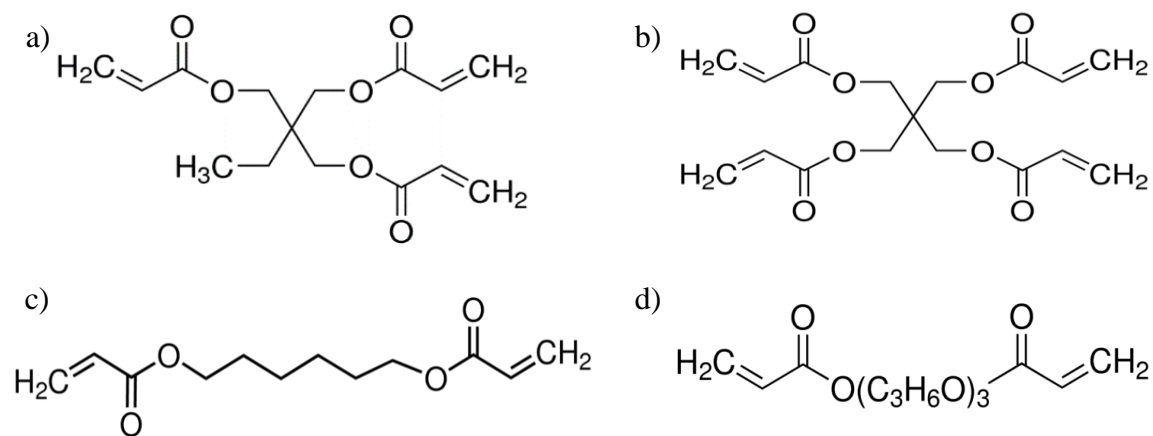
Figure 17. Structures of diluent monomers for a) TMPTA, b) PETA, c) HDDA, and d) TPGDA.

Formulations were prepared by directly combining the desired AECO (or DMECO), initiator, and diluent by weight ratios into a plastic beaker on a Cole-Parmer digital scale. Each was mixed until a homogenous mixture was obtained ($\approx$2min) by an IKA RW20 standing mixer before being centrifuged at 2000 rpm for 5min to remove air bubbles. A variety of formulations were trialed as shown in *Table 5* to comprehensively study each's capabilities. Each formulation is denoted first with the oil to diluent content weight ratio followed by the type of oil. TPGDA was used first as the reactive diluent at different resin/diluent ratios. The other three diluents were tested at the 65/30 resin to diluent ratio. To limit initiator decomposition over time, formulations were stored in a refrigerator when not being used. Formulations containing AESO were prepared for comparison.

Table 5. Formulations for the samples based on AECO, AESO, and DMECO resins.

Formulation	AECO (wt%)	AESO (wt%)	Diluent (wt%)	Initiator (wt%)	Base Constituent
95-0 AECO	95%		0%		
85-10 AECO	85%		10%		
75-20 AECO	75%	0%	20%	5%	Cottonseed oil
65-30 AECO	65%		30%		
55-40 AECO	55%		40%		
45-50 AECO	45%		50%		
AECO HDDA					
AECO PETA	65%	0%	30%	5%	Cottonseed oil
AECO TMPTA					
DMECO TPGDA					
95-0 AESO		95%	0%		
85-10 AESO	0%	85%	10%	5%	Soybean oil
65-30 AESO		65%	30%		

Sample Preparation

As shown in *Figure 18*, each tensile sample was prepared by pouring the desired formulation across a 0.5-mm deep silicone mold designed according to the ASTM D882 standard for thin film tensile testing. To purge air bubbles and excess resin, a glass plate was gradually laid on top of the mold. A 20W 405nm UV lamp was then placed on top of the glass plate (6-mm distance between the lamp and sample surface) and was turned on for 2-min. Next the lamp and silicone mold were removed leaving the tensile bars adhered to the glass plate. After careful removal using a razor, the tensile samples were briefly rinsed with isopropyl alcohol to remove excess uncured resin and were stored in a zip-lock bag.

Figure 18. Manufacturing procedure for tensile samples.

Dynamic mechanical analysis (DMA) bar samples were prepared in a similar fashion to the above tensile samples, however instead of immediately placing the samples in a zip-lock bag they were instead laid in an atmospheric chamber under ambient temperature and pressure overnight to condition the samples before testing as seen in *Figure 19*.

Figure 19. A variety of DMA bars conditioning in an atmospheric chamber.

Characterization Results

Tensile Testing

Tensile testing was conducted on a Instron 5545 tensile tester at 5mm/min for a variety of different formulations as shown in *Figure 20 & 21* with data tabulate in *Tables 6 & 7*.

Formulation ratios for each resin are specified first with the oil used followed by the percent weight of oil and diluent (e.g. AECO 85-10 has 85 wt% AECO, 10 wt% diluent, and 5 wt% photo initiator). Formulations without a specified ratio are 65 wt% oil and 30% diluent of which is specified in the name. For the AECO formulations, the tensile strength and modulus of the samples increased with the content of the reactive diluent TPGDA. This is most likely due to the diluent's higher number of functionality than AECO, which results in its higher crosslinking density. While the strength and rigidity of the samples improved, the ultimate strain fluctuated within the tested diluent content without showing significant decreases. TPGDA has the lowest functionality among the four reactive diluents. Replacing TPGDA with HDDA, TMPTA, or PETA led to higher strength and modulus of the samples due to the higher functionality of the latter.
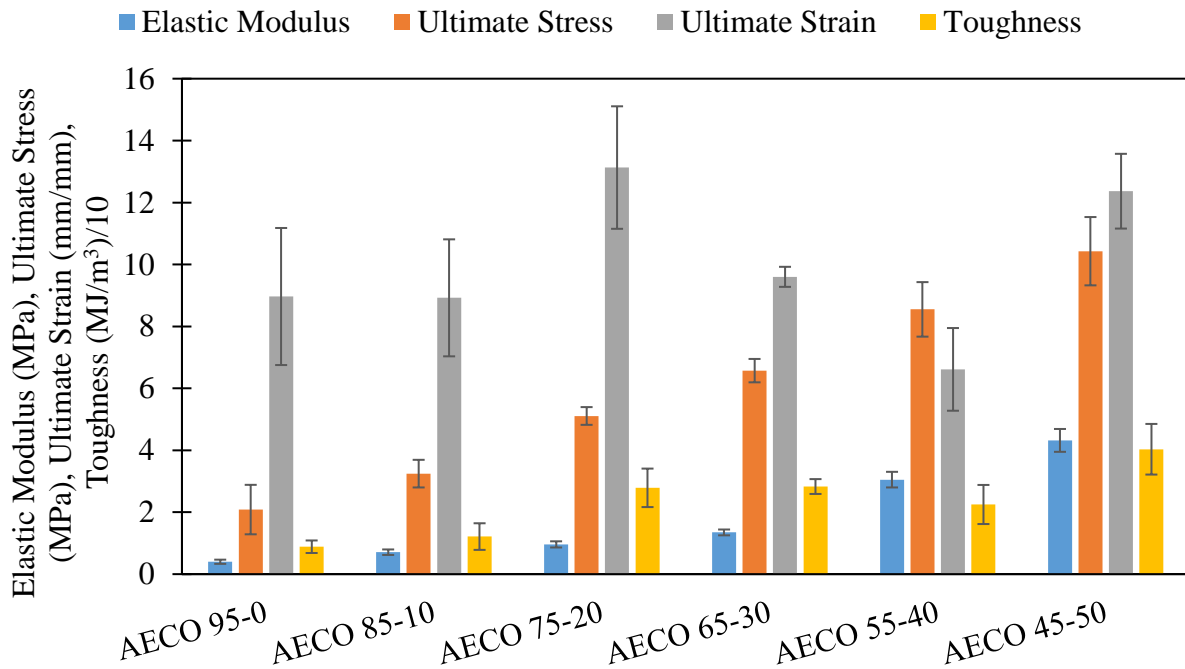
Figure 20. Tensile properties of AECO formulations containing TPGDA reactive diluent.

Table 6. Tensile properties of AECO formulations containing TPGDA reactive diluent.

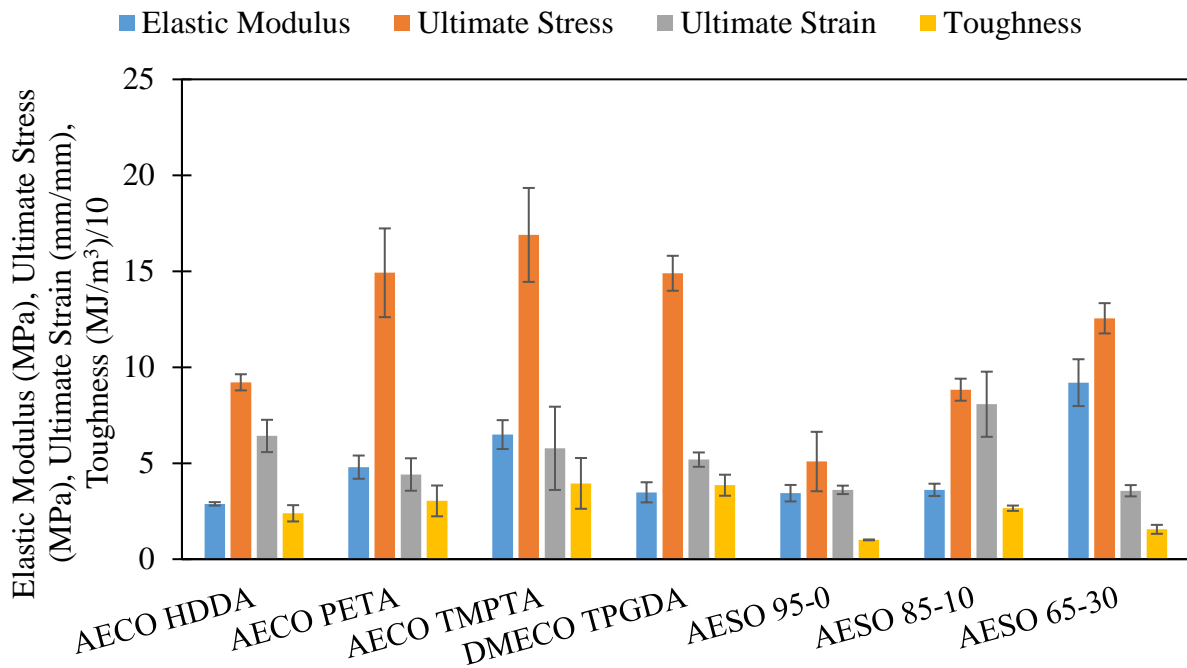| Tensile Properties	AECO 95-0	AECO 85-10	AECO 75-20	AECO 65-30	AECO 55-40	AECO 45-50
Elastic Modulus (MPa)	0.4 ±0.067	0.71 ±0.086	0.96 ±0.1	1.35 ±0.095	3.05 ±0.252	4.32 ±0.369
Ultimate Stress (MPa)	2.09 ±0.8	3.25 ±0.446	5.11 ±0.287	6.57 ±0.378	8.55 ±0.88	10.4 ±1.1
Ultimate Strain (mm/mm)	8.97 ±2.21	8.92 ±1.89	13.1 ±1.98	9.6 ±0.324	6.61 ±1.33	12.4 ±1.21
Toughness (MJ/m^3)	8.85 ±2.02	12.1 ±4.3	27.9 ±6.21	28.3 ±2.4	22.5 ±6.31	40.3 ±8.18

Figure 21. Tensile properties of AECO, DMECO, and AESO formulations*.

Table 7. Tensile properties of AECO, DMECO, and AESO formulations*.

Tensile Properties	AECO HDDA	AECO PETA	AECO TMPTA	DMECO TPGDA	AESO 95-0	AESO 85-10	AESO 65-30
Elastic Modulus (MPa)	2.88 ±0.089	4.8 ±0.605	6.49 ±0.752	3.48 ±0.526	3.44 ±0.43	3.61 ±0.321	9.2 ±1.22
Ultimate Stress (MPa)	9.22 ±0.421	14.9 ±2.31	16.9 ±2.45	14.9 ±0.911	5.09 ±1.55	8.83 ±0.574	12.6 ±0.788
Ultimate Strain (mm/mm)	6.42 ±0.842	4.41 ±0.846	5.78 ±2.17	5.19 ±0.373	3.61 ±0.219	8.07 ±1.7	3.57 ±0.294
Toughness (MJ/m^3)	23.9 ±4.24	30.4 ±8.03	39.5 ±13.2	38.5 ±5.48	10.1 ±0.219	26.6 ±1.38	15.5 ±2.34

* Resin to reactive diluent ratio is 65:30 for the AECO and DMECO formulations. TPGDA as the reactive diluent for AESO samples.

Comparing AECO to AESO samples in similar formulations using TPGDA as the reactive diluent, AESO samples showed higher strengths and moduli because of AESO's higher functionality. Each soybean oil molecule contains on average five C=C bonds available for epoxidation and subsequent acrylation while a cottonseed oil molecule only has three. Among the AESO samples, a higher reactive diluent content led to higher strengths and moduli of the samples; the same trend was observed among AECO samples. Dimethacrylation doubles the number of reactive groups in a resin molecule compared to acrylation. As a result, dimethacylated resin should show a higher strength and modulus than a similarly formulated acrylated sample. This trend can be clearly observed by comparing the properties of the AECO-TPGDA and DMECO-TPGDA samples.

Dynamic Mechanical Analysis

DMA testing was conducted on a TA Q850 DMA while sample preparation followed previous works for DMA samples. By dividing the loss modulus by the storage modulus, tan(δ) could be calculated which was used to estimate the T_g of each formulation. In *Figure 22*, the peak value of each curve denotes the rough T_g for the respective material. Formulation 95-0

AECO exhibits a T_g averaging much lower than that of 95-0 AESO which could be caused by the lower average functionality in AECO, which resulted in its lower crosslinking density. A similar difference in T_g can also be seen between 85-10 AECO and 85-10 AESO. Introduction of diluent into the natural oils displays an increase in glass transition temperature of 1.2 and 8.2°C for AECO and AESO, respectively. The breadth of the peaks for the AECO samples appeared to be larger than those of the AESO samples, indicating higher inhomogeneity of the crosslinking density in the former.
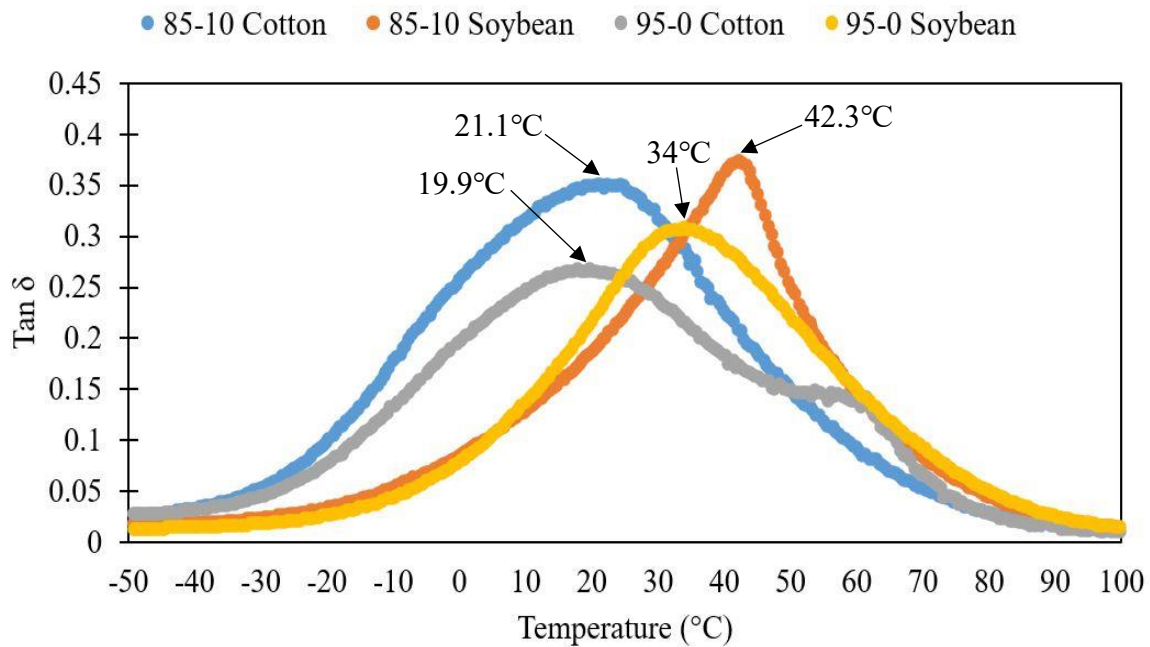
Figure 22. Tan(δ) of AECO and AESO formulations containing TPGDA.

Additive Manufacturing

Stereolithography 3D Printing

Stereolithography has become a well-known and promising technique for manufacturing small, detailed objects out of UV-curable commercial resins. With the incorporation of a photo initiator into the AECO, it too could be used in an SLA printer to print structures. A Moai 130 SLA printer was utilized with upgraded build plate and resin vat. Displayed in *Figure 23* is the

general processing for printing with the object adhered to the build plate after printing, sitting on a solar powered rotating table in a UV post-curing chamber, and the printed object before and after model support removal.
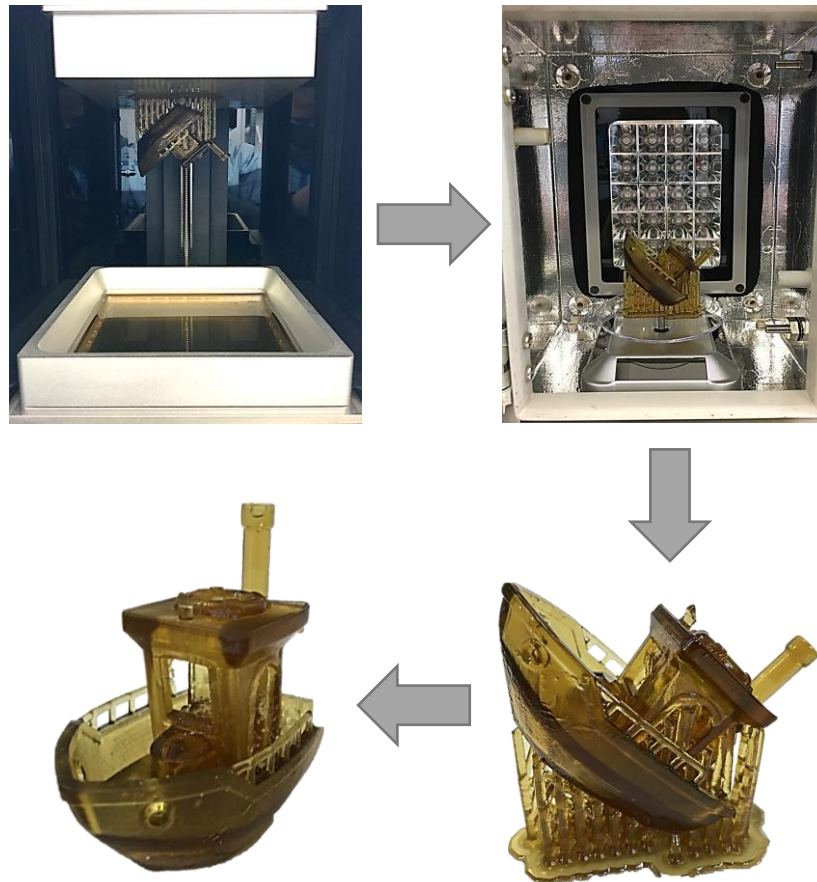
Figure 23. Process for printing a model (Benchy) using AECO 55-40 resin.

Through trialing, it was found that repeatable and accurate objects could only be made with formulations containing at most 55% AECO due to a couple reasons. At a higher content of AECO, the larger viscosity occasionally inhibited the resin from flowing quick enough underneath the object to form the next layer. While this could be negated by using a large quantity of resin, the overall adhesion of high-AECO-content formulations to the build plate was poor and would lead to objects being either adhered to or floating loosely in the resin vat. For

these reasons, the 55-40 AECO formulation was used predominantly to print objects as seen in

Figure 24.

Figure 24. 3D printed ring, Benchy, and glasses temple models with 55% AECO formulation.

Post Curing

Two methods of post-curing (i.e. UV and thermal) were investigated as seen in *Figure 25*

after printing due to noticeable degradation of printed objects in preliminary UV post-cures. Both

methods involved N_2 gas environments to eliminated oxygen inhibition on the surface of the

objects. Oxygen inhibition is a notorious problem with resin printing where radical oxygen atoms

in the atmosphere will overtake the monomer bonding on the object surface and form a 1-3μm

thick tacky layer of uncured resin at the air interface. Similar to the curing of testing specimens,

a 20W UV LED lamp was used for UV post-cure whereas a quartz tube furnace was used to

thermally post-cure after printing. To achieve thermal post-curing, a thermal initiator had to be

added to the AECO formulation. At a concentration of 5wt%, the thermal initiator replaced

5wt% of the diluent in the 55-40 AECO formulation reducing the diluent content 35wt%. Prior to

post-curing, each print was rinsed briefly in both a primary and secondary isopropyl bath to remove most excess uncured resin and remaining support material. After a pat dry and resting in an ambient air environment for 30min, each object displayed smooth uniform structures with mild flexibility, a tacky surface, and a slight chemical odor. Once dry, the objects were placed in their respective post-curing chambers and let rest for 5min to ensure a complete N_2 environment.
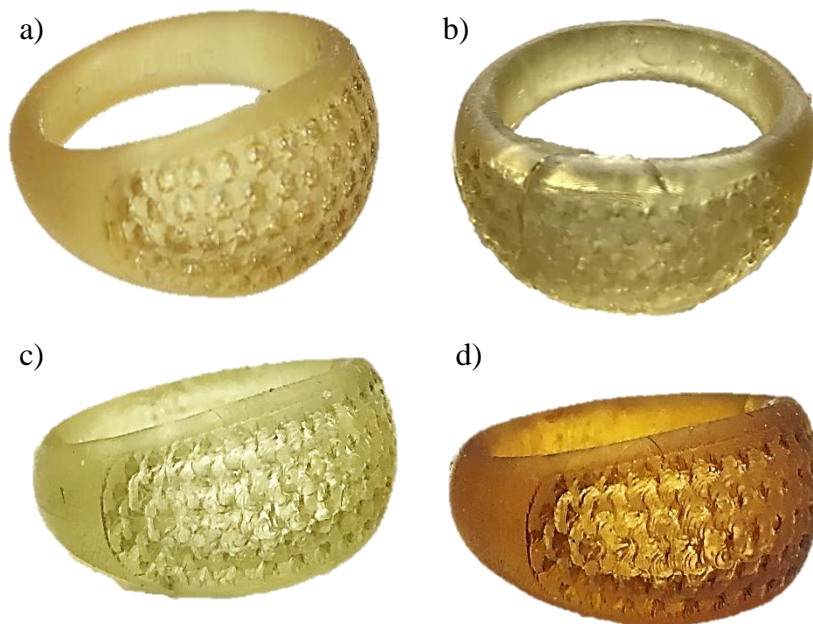
Figure 25. 3D printed AECO rings under different post-curing conditions: a) uncured, b) 2min UV cured, c) 2hr 100°C thermally cured, and d) 2hr 200°C thermally cured.

After post-curing, significant differences can be seen between each post-curing method and parameter. UV curing for only 2min is seen to cause dramatic cracks to propagate through the structure likely caused by internal stress buildup due to the curing/shrinking on the surface layer of the structure. Objects cured by UV for under 2min displayed less cracking, however the undesirable tacky surface and chemical odor were still present. Flexibility of the structure was slightly reduced during the UV post-curing but was superseded by the observed increase in rigidity when compressed by hand. To improve upon these issues, thermal post-curing was experimented. Preliminary tests showed little effect on the samples when cured at between 100-

200°C for 1hr besides slightly less tackiness after the 200°C treatment. Increasing the duration of treatment to 2hrs however showed significant alterations, most notably the color changing from golden to amber. After 100°C for 2hrs, some surface tackiness remained however the odor was nearly completely diminished, no visible cracks formed, and the rigidity displayed was comparable to the 2min UV cured sample. After 200°C for 2hrs, all tackiness and odor were eliminated, however some minor cracks formed but with little propagation. Of all samples, the 200°C for 2hrs displayed the largest increase in rigidity which is understandable because thermal post-curing cures the entire objects volume whereas UV can only penetrate a few microns into the objects surface. Thermal post-curing under elevated temperatures also allows polymer chain relaxation and therefore reduces/eliminates internal stress buildup, decreasing the probability of sample cracking.

Discussion

Being that cottonseed oil is comprised of one glycerol molecule hinged to three fatty acids similar to other natural oils, chemical modification was possible as seen in previous studies. Chemically, the only part of the natural oils effected during the acrylation and epoxidation stages is their unsaturated double bonds which are broken to form reactive sites. Each natural oil is attributed a specific degree of unsaturation based on the average types of fatty acids that comprise them. CSO has been found to have on average 78% unsaturated fatty acids compared to 84%, 89%, and 97% in soybean, sunflower and castor oil respectively.[49,50] Some of the unsaturated fatty acids are mono-unsaturated while other poly-unsaturated with distributions varying dramatically between natural oils. Soybean oil specific has only marginally greater unsaturation with distributions of mono- to poly-unsaturated fats comparable to that of CSO.[49] AESO outperformed AECO in all tested properties except ultimate strain using the same type

53

and contents of diluent and photo initiator as seen in *Figures 20 & 21*. Structurally the AECO is not forming as strong of a crosslinked network due to insufficient bonding likely induced by its lower degree-of-unsaturation.

Incorporation of reactive diluents into acrylated epoxidized oils is commonly done to improve mechanical strength and lower viscosity.[51] Diluents are typically petroleum derived and come in varying degrees of functionality from mono- to poly- with sizes ranging from simple monomer to short oligomers.[52] Most commonly used diluents have some form of acrylate groups at their ends to react when initiated as seen in *Figure 17*. Increasing diluent content in the AECO improved most properties until a deviation in trend is seen in the AECO 55-40 formulation. Similar deviation is seen with the AESO 65-30 formulation which could indicate incompatible ratios of resin to diluent where crosslinking is not ideal. Further increasing of diluent shows AECO 45-50 on trend with the previous samples illustrating an improved ratio.

Due to TPGDA having only two reactive acrylate groups and a long oligomer body, it has limited reactivity and a mild molecular weight of 300.35g/mol relative to the other diluents. Diluents with higher molecular weight and increased reactivity have been shown to increase bonding thereby improving mechanical properties.[52,53] Trials with HDDA showed promise for improvement in elastic modulus and ultimate stress with some sacrifice to ultimate strain and toughness compared to with TPGDA. Comparing the two diluents clearly shows a shorter oligomer body in HDDA which has a molecular weight of 226.27g/mol, hindering chain dislocation compared to longer oligomers such as TGPDA. Further trialing with TMPTA and PETA saw increases in all properties except ultimate strain compared to HDDA which can be expected when increasing the acrylate groups available. While PETA and TMPTA have four and three reactive sites, respectively, TMPTA's lower molecular weight of 296.32g/mol compared to

54

PETA's 352.34g/mol caused by the replacement of one acrylate group with a methyl group appears to significantly improve properties. This could hypothetically be caused by increased homo-polymerization with PETA due to its formulation containing a higher ratio of diluent to oil functional sights. Using TPDGA however, DMECO was able to achieve properties comparable to AECO TMPTA, indicating the superiority of the dimethacrylates due to its increased functionality. Comparing petroleum derived Siraya Simple SLA resin to AECO TMPTA displayed improvements in modulus, ultimate stress, ultimate strain, and toughness upwards of 2.6, 2.9, 1.5, and 3.5 times that of the latter. Further study must be done into increasing the potential of natural oil derived resins to display viability for the market.

Many studies are seeking to repurpose acrylated and epoxidized natural oils as plasticizers in existing polymers for copolymerization. Expectedly, nearly all studies have found a decrease in average glass transition temperature correlated to an increase in natural oil content.[36,37,54] It's been understood that these changes are attributed to increasing free volume allowing for improved chain mobility during deformation.[36] Similar trends can be seen in *Figure 22* where through the incorporation of just 10% diluent, increases in glass transition temperature occur for both AECO and AESO. Greater increase in AESO may be attributed to its higher functionality allowing for superior initial improvement when introduced to diluent. Difference in functionality likely also attributes to the wider transition region of AECO compared to AESO which has better defined peaks.

Culminated from the mechanical data was the successful application of AECO-based resin as SLA 3D printable material. Numerous works have shown this to be possible with a variety of other natural oils both with and without diluent.[38,39,55] While repeatable successful objects could only be manufactured with AECO 55-45 due to AECO's high viscosity and dark

hue. Use of different diluents or photo initiators as explored by others could be trialed to allow increased AECO content of 3D printable resins. As it stands however, 3D printing complex structures used for the calibration of standard 3D printing materials as seen in *Figure 24* is possible with sharp and well-defined corners and edges.

Post-curing is typically a requirement for SLA 3D printed objects being that the outer layers are coated in uncured resin after manufacturing. Common methods utilized intense but brief exposure to UV light due to the already incorporated photo initiator.[38,39] Trialing using a 20W UV lamp initially saw poor removal of the tacky surface on the printed objects after just 2min exposure. Oxygen inhibition is a known effect where radical oxygen in the air will bond to micron thick layers of resin as it photolitically activates thus impeding the crosslinking. [56] Replacing the air environment with N_2 immediately relieved the tackiness, however in either environment degradation was seen. This is evident of chain scission and surface tension forming as new bonds form which causes extreme crack propagation.[57] With no combination of post curing duration and environment offering promise, trials using thermal initiators for post-curing were instead sought. Promising results such as the removal of tackiness, loss of odor, improved rigidity, reduced degradation, and potential for controllable color alteration were seen with variable temperature and time curing combinations. Reduced degradation is likely influenced by the more gradual curing expected of thermal initiators and the more volumetric relaxation in thermal environments compared to ambient.

Conclusion

The concept of AECO as an SLA 3D printable resin was presented through the incorporation of a diluent as well as a photo and thermal initiator. Evidence from previous studies displayed the potential with AESO giving a clear idea of benefits and detriments.

Mechanical properties suggested the AECO cannot form as strong of a crosslinked structure as AESO, however modification to form DMECO greatly enhances the CSO's potential. Explanation for these properties is due to differing functionalities between the natural oils as well as their compatibility at varying ratios. Different diluents offered significantly different results attributing to their reactivity and molecular weight with TMPTA seemingly being most mechanically beneficial. Introduction of diluent increased the glass transition temperature as well but only by a slight degree for AECO. SLA 3D printing was enabled with AECO 55-45 due to the oil's high viscosity and allowed for objects with complex architectures to be manufactured. From this work it can be discernibly said that AECO processes the ability to be used as a 3D printable resin with further work needed to refine the mechanical properties and post-curing conditions.

CONCLUSIONS AND FUTURE WORK

Conclusions

Cotton is a renewable product that will continue to have influence in humankind's daily life for at least centuries to come. Current consumption however plagues our landfills as growing waste procures from the abundant applications requiring cotton products. In this thesis, application development to increase cotton product/waste value was sought for both cotton fabric as well as cottonseed oil through the means of thermal treatment for reinforcement of epoxy and as an SLA 3D printable resin, respectively.

Through furnace and autoclave treatments, the mechanical properties of cotton fabrics were changed dramatically with little reinforcement capabilities found from treatments above 180°C in autoclave and above 600°C in furnace due to crystalline cellulose degradation and an amorphous carbon structure, respectively. Low temperatures above 140°C in air and 180°C in N_2 for furnace treatments offered the most mechanical improvement due to oxidation in air and dehydration in both air and N_2 which improved hydrophobicity and increased interfacial friction. Together, this proves the potential of thermally treated cotton fabrics as tailorable reinforcement in crosslinked polymer matrices.

After acrylation and epoxidation of CSO, combination with a photo initiator and diluent allowed for effective SLA 3D printing. Mechanical tests expectedly showed lower properties for AECO in comparison to AESO due to AECO's lower functionality. However, through the incorporation of diluents with different molecular weights and reactivity, properties were found to improve tremendously with TMPTA offering ideal copolymerization. Implementing DMECO however showed properties superior to that of AESO due to the added functionality. Successful and repeatable SLA 3D printing was accomplished with resins containing up to 55 wt% AECO

due to the oil's high viscosity. Initial attempts to UV post-cure objects resulted in degradation, residual tackiness, and noticeable odor. Utilizing an N_2 reduced odor significantly and removed tackiness, however degradation was still present. Incorporation of a thermal initiator allowed for thermal post curing in N_2 which displayed the removal of tackiness, loss of odor, improved rigidity, reduced degradation, and potential for controllable color alteration. These results prove the potential for further development of CSO as an SLA 3D printable resin.

Future Work

Cotton Fabric

- Furnace treatment from 200°C to 600°C in both air and N_2 environments should be explored to encompass a complete understanding of potentially idea property ranges.
- Deeper analysis into the true extent of cellulose degradation with varying treatments using SEM, FTIR, and XRD to identify wall cleavage, changes in bond structures, and crystallinity degradation.

Cottonseed Oil

- More diluent formulations and blends should be trialed to determine idea ratios for improved properties and increased AECO incorporation for 3D printing.
- Further DMECO study with different diluents should be sought due to its significantly improved properties of AECO.
- Deeper analysis of resin formulations using rheology to understand the viscoelastic properties with added diluents and SEM for analysis of fracture surface modes and degradation to 3D printed parts.

REFERENCES

(1)   United Nations Conference on Trade and Development. From Fibre to Fabric Celebrating the Value of Cotton. *Online Publication*. **2019**. https://unctad.org/news/fibre-fabric-celebrating-value-cotton.

(2)   Moulherat, C.; Tengberg, M.; Haquet, J.-F.; Mille, B. First Evidence of Cotton at Neolithic Mehrgarh, Pakistan: Analysis of Mineralized Fibres from a Copper Bead. *J. Archaeol. Sci.* **2002**, *29* (12), 1393–1401. https://doi.org/10.1006/jasc.2001.0779.

(3)   Serra, A.; Tarrés, Q.; Llop, M.; Reixach, R.; Mutjé, P.; Espinach, F. X. Recycling Dyed Cotton Textile Byproduct Fibers as Polypropylene Reinforcement. *Text. Res. J.* **2019**, *89* (11), 2113–2125. https://doi.org/10.1177/0040517518786278.

(4)   Asaadi, S.; Hummel, M.; Hellsten, S.; Härkäsalmi, T.; Ma, Y.; Michud, A.; Sixta, H. Renewable High-Performance Fibers from the Chemical Recycling of Cotton Waste Utilizing an Ionic Liquid. *ChemSusChem* **2016**, *9* (22), 3250–3258. https://doi.org/10.1002/cssc.201600680.

(5)   Baccouch, W.; Ghith, A.; Yalcin-Enis, I.; Sezgin, H.; Miled, W.; Legrand, X.; Faten, F. Enhancement of Fiber-Matrix Interface of Recycled Cotton Fibers Reinforced Epoxy Composite for Improved Mechanical Properties. *Mater. Res. Express* **2020**, *7* (1), 015340. https://doi.org/10.1088/2053-1591/ab6c04.

(6)   Deng, C.; Pan, L.; Cui, R.; Li, C.; Qin, J. Wearable Strain Sensor Made of Carbonized Cotton Cloth. *J. Mater. Sci. Mater. Electron.* **2017**, *28* (4), 3535–3541. https://doi.org/10.1007/s10854-016-5954-7.

(7)   Paksung, N.; Pfersich, J.; Arauzo, P. J.; Jung, D.; Kruse, A. Structural Effects of Cellulose on Hydrolysis and Carbonization Behavior during Hydrothermal Treatment. *ACS Omega* **2020**, *5* (21), 12210–12223. https://doi.org/10.1021/acsomega.0c00737.

(8)   Sharma, A.; Kodgire, P.; Kachhwaha, S. S. Biodiesel Production from Waste Cotton-Seed Cooking Oil Using Microwave-Assisted Transesterification: Optimization and Kinetic Modeling. *Renew. Sustain. Energy Rev.* **2019**, *116*, 109394. https://doi.org/10.1016/j.rser.2019.109394.

(9)   Carbonell-Verdu, A.; Garcia-Garcia, D.; Dominici, F.; Torre, L.; Sanchez-Nacher, L.; Balart, R. PLA Films with Improved Flexibility Properties by Using Maleinized Cottonseed Oil. *Eur. Polym. J.* **2017**, *91*, 248–259. https://doi.org/10.1016/j.eurpolymj.2017.04.013.

(10)   Carbonell-Verdu, A.; Bernardi, L.; Garcia-Garcia, D.; Sanchez-Nacher, L.; Balart, R. Development of Environmentally Friendly Composite Matrices from Epoxidized Cottonseed Oil. *Eur. Polym. J.* **2015**, *63*, 1–10. https://doi.org/10.1016/j.eurpolymj.2014.11.043.

(11)   Johnson, J.; Lanclos, K.; MacDonald, S.; Meyer, L.; Soley, G. The World and United States Cotton Outlook. *USDA Agricultural Outlook Forum. Online Publication*. **2020**. https://www.usda.gov/sites/default/files/documents/Cotton.pdf

(12)   Ismal, Ozlenen. Influence of Wax and Pectin Removal on Cotton Absorbency. *International Magazine for Textile Professionals*. 2008, *8* (6), pp 3.

(13)   Kozłowski, R. M.; Mackiewicz-Talarczyk, M. 1A - Introduction to Natural Textile Fibres. In *Handbook of Natural Fibres (Second Edition)*; Kozłowski, R. M., Mackiewicz-Talarczyk, M., Eds.; Woodhead Publishing Series in Textiles; Woodhead Publishing, 2020; pp 1–13. https://doi.org/10.1016/B978-0-12-818398-4.00001-3.

(14)   Dochia, M.; Sirghie, C.; Kozlowski, R. M.; Roskwitalski, Z. Cotton Fibres. In *Handbook of Natural Fibres*; Woodhead Publishing, 2012; Vol. 1, pp 11–23.

(15)   Wakelyn, P. J.; Bertoniere, N. R.; French, A. D.; Thibodeaux, D. P.; Triplett. B, A.; Rousselle, M.; Goynes, W. R.; Edwards, J. V.; Hunter, L.; McAlister, D. D.; Gamble, G. R. Cotton Fiber Chemistry and Technology. *International Fiber Science and Science*. **2007**, pp 170.

(16)   Liu, W.; Liu, S.; Liu, T.; Liu, T.; Zhang, J.; Liu, H. Eco-Friendly Post-Consumer Cotton Waste Recycling for Regenerated Cellulose Fibers. *Carbohydr. Polym.* **2019**, *206*, 141–148. https://doi.org/10.1016/j.carbpol.2018.10.046.

(17)   Hashmi, S. A. R.; Dwivedi, U. K.; Chand, N. Friction and Sliding Wear of UHMWPE Modified Cotton Fibre Reinforced Polyester Composites. *Tribol. Lett.* **2006**, *21* (2), 79–87. https://doi.org/10.1007/s11249-006-9014-y.

(18)   Moradi, E.; Zeinedini, A. On the Mixed Mode I/II/III Inter-Laminar Fracture Toughness of Cotton/Epoxy Laminated Composites. *Theor. Appl. Fract. Mech.* **2020**, *105*, 102400. https://doi.org/10.1016/j.tafmec.2019.102400.

(19)   Kamble, Z.; Behera, B. K.; Mishra, R.; Behera, P. K. Influence of Cellulosic and Non-Cellulosic Particle Fillers on Mechanical, Dynamic Mechanical, and Thermogravimetric Properties of Waste Cotton Fibre Reinforced Green Composites. *Compos. Part B Eng.* **2021**, *207*, 108595. https://doi.org/10.1016/j.compositesb.2020.108595.

(20)   Battegazzore, D.; Frache, A.; Abt, T.; Maspoch, M. L. Epoxy Coupling Agent for PLA and PHB Copolymer-Based Cotton Fabric Bio-Composites. *Compos. Part B Eng.* **2018**, *148*, 188–197. https://doi.org/10.1016/j.compositesb.2018.04.055.

(21)   Izadyar, S.; Aghabozorgi, M.; Azadfallah, M. Palmitic Acid Functionalization of Cellulose Fibers for Enhancing Hydrophobic Property. *Cellulose* **2020**, *27* (10), 5871–5878. https://doi.org/10.1007/s10570-020-03174-x.

(22)   Mai, Z. Multifunctionalization of Cotton Fabrics with Polyvinylsilsesquioxane/ZnO Composite Coatings. *Carbohydr. Polym.* **2018**, 10.

(23)   Yu, Y.; Wu, H. Significant Differences in the Hydrolysis Behavior of Amorphous and Crystalline Portions within Microcrystalline Cellulose in Hot-Compressed Water. *Ind. Eng. Chem. Res.* **2010**, *49* (8), 3902–3909. https://doi.org/10.1021/ie901925g.

(24)   Deguchi, S.; Tsujii, K.; Horikoshi, K. Crystalline-to-Amorphous Transformation of Cellulose in Hot and Compressed Water and Its Implications for Hydrothermal Conversion. *Green Chem* **2008**, *10* (2), 191–196. https://doi.org/10.1039/B713655B.

(25)   García-Bordejé, E.; Pires, E.; Fraile, J. M. Parametric Study of the Hydrothermal Carbonization of Cellulose and Effect of Acidic Conditions. *Carbon* **2017**, *123*, 421–432. https://doi.org/10.1016/j.carbon.2017.07.085.

(26)   Xu, Z.; Qi, R.; Xiong, M.; Zhang, D.; Gu, H.; Chen, W. Conversion of Cotton Textile Waste to Clean Solid Fuel via Surfactant-Assisted Hydrothermal Carbonization: Mechanisms and Combustion Behaviors. *Bioresour. Technol.* **2021**, *321*, 124450. https://doi.org/10.1016/j.biortech.2020.124450.

(27)   Mauter, M. S.; Elimelech, M. Environmental Applications of Carbon-Based Nanomaterials. *Environ. Sci. Technol.* **2008**, *42* (16), 5843–5859. https://doi.org/10.1021/es8006904.

(28)   Zheng, Y.; Li, Y.; Zhou, Y.; Dai, K.; Zheng, G.; Zhang, B.; Liu, C.; Shen, C. High-Performance Wearable Strain Sensor Based on Graphene/Cotton Fabric with High Durability and Low Detection Limit. *ACS Appl. Mater. Interfaces* **2020**, *12* (1), 1474–1485. https://doi.org/10.1021/acsami.9b17173.

(29)   Li, L.; Zhong, Q.; Kim, N. D.; Ruan, G.; Yang, Y.; Gao, C.; Fei, H.; Li, Y.; Ji, Y.; Tour, J. M. Nitrogen-Doped Carbonized Cotton for Highly Flexible Supercapacitors. *Carbon* **2016**, *105*, 260–267. https://doi.org/10.1016/j.carbon.2016.04.031.

(30)   Hong, X.; Li, S.; Wang, R.; Fu, J. Hierarchical SnO2 Nanoclusters Wrapped Functionalized Carbonized Cotton Cloth for Symmetrical Supercapacitor. *J. Alloys Compd.* **2019**, *775*, 15–21. https://doi.org/10.1016/j.jallcom.2018.10.099.

(31)   Bhattacharjee, P.; Singhal, R. S.; Tiwari, S. R. Supercritical Carbon Dioxide Extraction of Cottonseed Oil. *J. Food Eng.* **2007**, *79* (3), 892–898. https://doi.org/10.1016/j.jfoodeng.2006.03.009.

(32)   Saxena D. K.; Sharma, S.; Sambi, S. Comparative Extraction of Cottonseed Oil by N-Hexane and Ethanol. *Chemistry*. **2011**, *6* (1), pp 6.

(33)   Falaras, P.; Kovanis, I.; Lezou, F.; Seiragakis, G. Cottonseed Oil Bleaching by Acid-Activated Montmorillonite. 12.

(34)   Yang, A.; Qi, M.; Wang, X.; Wang, S.; Sun, L.; Qi, D.; Zhu, L.; Duan, Y.; Gao, X.; Ali Rajput, S.; Zhang, N. Refined Cottonseed Oil as a Replacement for Soybean Oil in Broiler Diet. *Food Sci. Nutr.* **2019**, *7* (3), 1027–1034. https://doi.org/10.1002/fsn3.933.

(35)   Sinha, D.; Murugavelh, S. Biodiesel Production from Waste Cotton Seed Oil Using Low Cost Catalyst: Engine Performance and Emission Characteristics. *Perspect. Sci.* **2016**, *8*, 237–240. https://doi.org/10.1016/j.pisc.2016.04.038.

(36)   Carbonell-Verdu, A.; Samper, M. D.; Garcia-Garcia, D.; Sanchez-Nacher, L.; Balart, R. Plasticization Effect of Epoxidized Cottonseed Oil (ECSO) on Poly(Lactic Acid). *Ind. Crops Prod.* **2017**, *104*, 278–286. https://doi.org/10.1016/j.indcrop.2017.04.050.

(37)   Carbonell-Verdu, A.; Garcia-Sanoguera, D.; Jordá-Vilaplana, A.; Sanchez-Nacher, L.; Balart, R. A New Biobased Plasticizer for Poly(Vinyl Chloride) Based on Epoxidized Cottonseed Oil. *J. Appl. Polym. Sci.* **2016**, *133* (27). https://doi.org/10.1002/app.43642.

(38)   Cui, Y.; Yang, J.; Lei, D.; Su, J. 3D Printing of a Dual-Curing Resin with Cationic Curable Vegetable Oil. *Ind. Eng. Chem. Res.* **2020**, *59* (25), 11381–11388. https://doi.org/10.1021/acs.iecr.0c01507.

(39)   Barkane, A.; Platnieks, O.; Jurinovs, M.; Gaidukovs, S. Thermal Stability of UV-Cured Vegetable Oil Epoxidized Acrylate-Based Polymer System for 3D Printing Application. *Polym. Degrad. Stab.* **2020**, *181*, 109347. https://doi.org/10.1016/j.polymdegradstab.2020.109347.

(40)   Łojewska, J.; Miśkowiec, P.; Łojewski, T.; Proniewicz, L. M. Cellulose Oxidative and Hydrolytic Degradation: In Situ FTIR Approach. *Polym. Degrad. Stab.* **2005**, *88* (3), 512–520. https://doi.org/10.1016/j.polymdegradstab.2004.12.012.

(41)   Ahn, K.; Zaccaron, S.; Zwirchmayr, N. S.; Hettegger, H.; Hofinger, A.; Bacher, M.; Henniges, U.; Hosoya, T.; Potthast, A.; Rosenau, T. Yellowing and Brightness Reversion of Celluloses: CO or COOH, Who Is the Culprit? *Cellulose* **2019**, *26* (1), 429–444. https://doi.org/10.1007/s10570-018-2200-x.

(42)   Scheirs, J.; Camino, G.; Tumiatti, W. Overview of Water Evolution during the Thermal Degradation of Cellulose. *Eur. Polym. J.* **2001**, *37* (5), 933–942. https://doi.org/10.1016/S0014-3057(00)00211-1.

(43)   Paquet, O.; Krouit, M.; Bras, J.; Thielemans, W.; Belgacem, M. N. Surface Modification of Cellulose by PCL Grafts. *Acta Mater.* **2010**, *58* (3), 792–801. https://doi.org/10.1016/j.actamat.2009.09.057.

(44)   El-Shishtawy, R. M.; Asiri, A. M.; Abdelwahed, N. A. M.; Al-Otaibi, M. M. In Situ Production of Silver Nanoparticle on Cotton Fabric and Its Antimicrobial Evaluation. *Cellulose* **2011**, *18* (1), 75–82. https://doi.org/10.1007/s10570-010-9455-1.

(45)   Steinbach, D.; Kruse, A.; Sauer, J.; Vetter, P. Sucrose Is a Promising Feedstock for the Synthesis of the Platform Chemical Hydroxymethylfurfural. *Energies* **2018**, *11* (3), 645. https://doi.org/10.3390/en11030645.

(46)   Shafizadeh, F. Thermal Degradation of Cellulose. *Cellul. Chem. Its Appl.* **1985**, 266–289.

(47)   Shafizadeh, F. Pyrolysis and Combustion of Cellulosic Materials; Wolfrom, M. L., Tipson, R. S., Eds.; Advances in Carbohydrate Chemistry; Academic Press, 1968; Vol. 23, pp 419–474. https://doi.org/10.1016/S0096-5332(08)60173-3.

(48)   Yang, H.; Gong, M.; Hu, J.; Liu, B.; Chen, Y.; Xiao, J.; Li, S.; Dong, Z.; Chen, H. Cellulose Pyrolysis Mechanism Based on Functional Group Evolutions by Two-Dimensional Perturbation Correlation Infrared Spectroscopy. *Energy Fuels* **2020**, *34* (3), 3412–3421. https://doi.org/10.1021/acs.energyfuels.0c00134.

(49)   Giakoumis, E. G. Analysis of 22 Vegetable Oils' Physico-Chemical Properties and Fatty Acid Composition on a Statistical Basis, and Correlation with the Degree of Unsaturation. *Renew. Energy* **2018**, *126*, 403–419. https://doi.org/10.1016/j.renene.2018.03.057.

(50)   Biopolymers, Alkyd Resins, Coatings. *Am. J. Polym. Sci.* **2013**, 10.

(51)   Chen, Z.; Wu, J. F.; Fernando, S.; Jagodzinski, K. Soy-Based, High Biorenewable Content UV Curable Coatings. *Prog. Org. Coat.* **2011**, *71* (1), 98–109. https://doi.org/10.1016/j.porgcoat.2011.01.004.

(52)   Demengeot, E.-A.-C.; Baliutaviciene, I.; Ostrauskaite, J.; Augulis, L.; Grazuleviciene, V.; Rageliene, L.; Grazulevicius, J. V. Crosslinking of Epoxidized Natural Oils with Diepoxy Reactive Diluents. *J. Appl. Polym. Sci.* **2010**, *115* (4), 2028–2038. https://doi.org/10.1002/app.31347.

(53)   Liu, C.; Wang, C.; Hu, Y.; Zhang, F.; Shang, Q.; Lei, W.; Zhou, Y.; Cai, Z. Castor Oil-Based Polyfunctional Acrylate Monomers: Synthesis and Utilization in UV-Curable Materials. *Prog. Org. Coat.* **2018**, *121*, 236–246. https://doi.org/10.1016/j.porgcoat.2018.04.020.

(54)   Grishchuk, S.; Karger-Kocsis, J. Hybrid Thermosets from Vinyl Ester Resin and Acrylated Epoxidized Soybean Oil (AESO). *Express Polym. Lett.* **2011**, *5* (1), 2–11. https://doi.org/10.3144/expresspolymlett.2011.2.

(55)   Skliutas, E.; Lebedevaite, M.; Kasetaite, S.; Rekštytė, S.; Lileikis, S.; Ostrauskaite, J.; Malinauskas, M. A Bio-Based Resin for a Multi-Scale Optical

3D Printing. *Sci. Rep.* **2020**, *10* (1), 9758. https://doi.org/10.1038/s41598-020-66618-1.

(56)   Ligon, S. C.; Husár, B.; Wutzel, H.; Holman, R.; Liska, R. Strategies to Reduce Oxygen Inhibition in Photoinduced Polymerization. *Chem. Rev.* **2014**, *114* (1), 557–589. https://doi.org/10.1021/cr3005197.

(57)   Behera, D.; Banthia, A. K. Synthesis, Characterization, and Kinetics Study of Thermal Decomposition of Epoxidized Soybean Oil Acrylate. *J. Appl. Polym. Sci.* **2008**, *109* (4), 2583–2590. https://doi.org/10.1002/app.28350.